Mustafa Samet PİR — CHARACTERIZATION OF NOVEL CILIARY GENE *TMEM145* — AGU 2020

CHARACTERIZATION OF NOVEL CILIARY GENE *TMEM145*

A THESIS
SUBMITTED TO THE DEPARTMENT OF BIOENGINEERING
AND THE GRADUATE SCHOOL OF ENGINEERING AND SCIENCE
OF ABDULLAH GUL UNIVERSITY
IN PARTIAL FULFILLMENT OF THE REQUIREMENTS
FOR THE DEGREE OF
MASTER

By
Mustafa Samet PİR
July 2020

CHARACTERIZATION OF NOVEL CILIARY GENE *TMEM145*

A THESIS
SUBMITTED TO THE DEPARTMENT OF BIOENGINEERING
AND THE GRADUATE SCHOOL OF ENGINEERING AND SCIENCE OF
ABDULLAH GUL UNIVERSITY
IN PARTIAL FULFILLMENT OF THE REQUIREMENTS
FOR THE DEGREE OF
MASTER OF SCIENCE

By
Mustafa Samet Pir
July 2020

SCIENTIFIC ETHICS COMPLIANCE

I hereby declare that all information in this document has been obtained in accordance with academic rules and ethical conduct. I also declare that, as required by these rules and conduct, I have fully cited and referenced all materials and results that are not original to this work.

Name-Surname: Mustafa Samet Pir
Signature :

REGULATORY COMPLIANCE

M.Sc. thesis titled "Characterization of Novel Ciliary Gene *tmem145*" has been prepared in accordance with the Thesis Writing Guidelines of the Abdullah Gül University, Graduate School of Engineering & Science.

Prepared By	Advisor
Mustafa Samet PİR	Dr. Öğr. Üyesi Oktay İsmail KAPLAN

Head of the Bioengineering Program
Prof. Dr. Sevil DİNÇER İŞOĞLU

ACCEPTANCE AND APPROVAL

M.Sc. thesis titled “Characterization of Novel Ciliary Gene *tmem145*” and prepared by Mustafa Samet PİR has been accepted by the jury in the Bioengineering Graduate Program at Abdullah Gül University, Graduate School of Engineering & Science.

…….. /…….. / ……..

(Thesis Defense Exam Date)

JURY:

Advisor : Dr. Öğr. Üyesi Oktay İsmail KAPLAN……

Member : Dr. Öğr. Üyesi Elif Nur FIRAT KARALAR……

Member : Dr. Öğr. Üyesi Aysun ADAN……

APPROVAL:

The acceptance of this M.Sc. thesis has been approved by the decision of the Abdullah Gül University, Graduate School of Engineering & Science, Executive Board dated ….. /….. / …….. and numbered ……..……. .

…….. /…….. / ……..

(Date)

Graduate School Dean
Prof. Dr. İrfan ALAN

ABSTRACT

CHARACTERIZATION OF NOVEL CILIARY GENE *TMEM145*

Mustafa Samet Pir
MSc. in Bioengineering
Supervisor: Dr. Oktay Ismail Kaplan

June 2020

Cilia and flagella are highly conserved, microtubule based cellular structures which are found in most of the organisms. They have variety of functions from enabling movement in protozoa to signal transduction in multi cellular organisms. Defects in the structure or the function of cilia in human cause a broad range of diseases called ciliopathies. These defects in cilia are caused by mutations on ciliary genes and some non-ciliary genes that affect function of cilia. Therefore, there is a constant need for new ciliary genes to be identified which may help reveal the molecular basis of ciliopathies. We have identified *C15A7.2*, a GPCR protein in *Caenorhabditis elegans* as a ciliary gene which is an ortholog of human *TMEM145* gene. We have investigated the function of *C15A7.2* encoding protein TMEM-145 and found decrease in the speed of intraflagellar transport system in *C15A7.2* mutant. We have not observed any structural defect in neither single nor various double mutants, implying that TMEM-145 is not required for ciliogenesis. Having localized exclusively in cilia, TMEM-145 is required to be further investigated.

Keywords: Cilia, ciliopathies, GPCR

ÖZET

YENİ BİR SİLYA GENİ OLAN *TMEM145*'İN KARAKTERİZASYONU

Mustafa Samet Pir

Biyomühendislik Bölümü Yüksek Lisans

Tez Yöneticisi: Dr. Oktay Ismail Kaplan

Haziran-2020

Silya ve flagella çoğu organizmada bulunan, mikrotübül yapılı, yüksek korunumlu hücresel bir yapıdır. Bunlar, protozoalarda hareket sağlamadan, çok hücreli canlılarda sinyal iletimine kadar bir çok fonksiyona sahiptir. Silyanın yapısında veya fonksiyonunda meydana gelen bozulmalar insanlarda silyopati denilen çeşitli hastalıklara sebep olur. Silyada meydana gelen bu bozukluklar silya genlerinde veya silya fonksiyonunu etkileyen silya geni olmayan genlerde meydana gelen mutasyonlardan kaynaklanır. Bu yüzden silyopatilerin moleküler temelini ortaya çıkarmaya yardımcı olacak yeni silya genleri keşfetmeye ihtiyaç vardır. GPCR proteini olan, insan *TMEM145* geninin ortoloğu olan ve *Caenorhabditis elegans*'ta bulunan *C15A7.2* genini silya geni olarak tanımladık. *C15A7.2* geni tarafından kodlanan TMEM-145 proteinin fonksiyonunu araştırdık ve *C15A7.2* mutantlarda intraflagellar transport sisteminin hızının yavaşladığını bulduk. Ne tekli, ne de çeşitli çiftli mutantlarda herhangi bir yapısal bozukluk gözlemlemedik. Bu da TMEM-145'in silya yapımında görev almadığını gösteriyor. Silyada bulunan bu genin tam fonksiyonunu öğrenmek için ilave analizler yapılmalıdır.

Anahtar kelimeler: Silya, silyopatiler, GPCR

Acknowledgements

I would like to first thank my supervisor Dr Oktay Kaplan, for his guidance and support during my M.Sc. I would like to thank Dr. Sebiha Çevik Kaplan for her support. I would like to thank all members of Kaplan lab for their help in my experiments, including Ferhan Yenisert especially for doing injections, Ziya Furkan Zorluer, Atiye Kılıç, Betül Altunkaynak and Merve Gül Turan for their help in experiments. I would like to thank my mom and dad for their life long support and lastly, I would like to thank my wife, Betül, for all her support inside and outside of the lab.

Table of Contents

1. INTRODUCTION 1

1.1. CILIA AND FLAGELLA 1

1.2. STRUCTURE OF CILIA 1

1.2.1. Ciliary axoneme 2

1.2.2. Transition zone 2

1.2.3. Distal region 3

1.3. THE CILIA IN *CAENORHABDITIS ELEGANS* 4

1.4. INTRAFLAGELLAR TRANSPORT SYSTEM 5

1.5. CILIOPATHIES 7

1.5.1. Primary Ciliary Dyskinesia 7

1.5.2. Polycystic Kidney Diseases 7

1.5.3. Sensory ciliopathies 8

1.6. G PROTEIN COUPLED RECEPTORS (GPCR) 9

1.7. CRISPR/CAS9 10

2. MATERIAL AND METHODS 12

2.1. MATERIALS 12

2.1.1. Strains 12

2.1.2. Primers and plasmids 14

2.2. METHODS 15

2.2.1. CRISPR/Cas9 gene editing 15

2.2.2. Microinjection in *C. elegans* 16

2.2.3. Worm maintenance and strains 18

2.2.4. Microscopic analysis 18

3. RESULTS 20

3.1. *C15A7.2* IS THE HOMOLOG OF HUMAN *TMEM145* GENE 20

3.2. TMEM-145 LOCALIZES ONLY IN CILIATED CELLS TO BOTH HEAD AND TAIL CILIA 22

3.3. TMEM-145 IS NOT NECESSARY FOR CILIOGENESIS 23

3.4. LOCALIZATIONS OF MEMBRANE PROTEINS ARE NOT DISRUPTED IN *TMEM-145(TUR002)* MUTANTS 29
3.5. DOUBLE MUTANT ANALYSIS 32
3.6. GENERATION OF NULL MUTANT ALLELE OF *TMEM-145* 33

4. DISCUSSION 36
5. CONCLUSIONS AND FUTURE PROSPECTS 40
5.1. CONCLUSIONS 40
5.2. CONTRIBUTION TO GLOBAL SUSTAINABILITY 40
5.3. FUTURE PROSPECTS 41

6. BIBLIOGRAPHY 43
7. APPENDIX 47

List of Figures

Figure 1.2.1 General structure of cilium 3

Figure 1.3.1 Life cycle of *C. elegans* 4

Figure 1.4.1 Intraflagellar transport system in *C. elegans* 6

Figure 1.5.1 Defects in cilia cause a wide range of diseases called ciliopathies 9

Figure 1.7.1 CRISPR/Cas systems 11

Figure 2.2.1.1 Schematic representation of Prb1017 plasmid 16

Figure 3.1.1 *C15A7.2* is the homolog of human *TMEM145* gene 21

Figure 3.2.1 TMEM-145 localizes to both head and tail cilia 22

Figure 3.3.1 *tmem-145(tur002)* allele has 666 bp deletion 23

Figure 3.3.2 Function of cilia in *tmem-145(tur002)* mutants are not defective 24

Figure 3.3.3 Localization of transition zone protein MKS-2 is not affected in *tmem-145(tur002)* mutants 25

Figure 3.3.4 *tmem-145(tur002)* mutation has no effect on PHA/B cilia structure and has no additive effect on ciliary defects in *arl-13* mutants 26

Figure 3.3.5 *tmem-145(tur002) mutation in C. elegans* does not rescue fan phenotype in AWB cilia of *grk-2* mutants 26

Figure 3.3.6 OLQ cilia have the same structure in *tmem-145(tur002)* mutants with wild type 27

Figure 3.3.7 OSM-6::GFP localization is not affected in *tmem-145* mutant worms but IFT is slower in *tmem-145(tur002)* mutants 29

Figure 3.4.1 C. elegans single *tmem-145(tur002)* mutants exhibit normal PKD-2 localization in CEM cilia in male worms 30

Figure 3.4.2 C. elegans single *tmem-145(tur002)* mutants show excess PKD-2 accumulation in CEM cilia in male worms 31

Figure 3.6.1 Schematic structure of *tmem-145(tur009)* allele 34

Figure 3.6.2 The structure of AWB cilia remains unaffected in *tmem-145(tur009)* allele 35

Dedication

For my wife, Betül

一番大切な人え。。

Chapter 1

Introduction

1.1 Cilia and Flagella

Cilia and flagella are highly conserved cellular structures found in a variety of species from protozoa to mammals. Although they are named differently at the time, when there was no evidence for both at the ultrastructural level, they are known to possess identical microtubule based structures [1]. We will use cilia and flagella interchangeably throughout this thesis. There are two types of cilia, motile and non-motile (primary) cilia. Cilia performs a variety of functions, for example, the unicellular alga *Chlamydomonas reinhardtii* uses flagella for motility; simply flagella is used to detect food using receptors on their surfaces to navigate the organisms to the stimulus [2]. Motile cilia can be present in human sperm and in embryonic nodes, which give the cell mobility. In some cases, motile cilia can be found on the epithelial cell surfaces as bundles, which help to move extracellular fluids [3]. On the other hand, non-motile (primary) cilia are found in almost all cell types in mammals, including olfactory neurons and photoreceptors [4]. These cilia are antenna like organelles emanating from cell surface, performing a variety of functions [5]. Cilia in kidney, for example, function as mechanosensory by helping kidney cells to divide properly by detecting fluid flow in the tubules while odorant sensing and photoreception are achieved by cilia of the olfactory and photosensory neurons, relaying extracellular message into the cell [6].

1.2 Structure of Cilia

1.2.1 Ciliary Axoneme

Ciliary structure consists of various sub compartments including basal body (BD), transition zone (TZ), periciliary membrane compartment (PCM), middle segment (MS), distal segment (DS) and tip of cilia.

The backbone of the cilia is a structure built on microtubules, called axoneme, which is the cilium skeleton. Ciliary axoneme consists of 9 doublet microtubules consisting of alpha and beta tubulins and surrounded by ciliary matrix and ciliary membrane [4]. In most of the motile cilia, two central microtubules are surrounded by 9 doublet microtubules forming 9+2 structure [7]. These cilia have inner and outer dynein arms generating the force for motility and this activity is regulated by radial spokes and central microtubule projections [4]. On the other hand, non-motile cilia are assembled from alpha and beta tubulins and have 9+0 microtubule structure lacking two central microtubules and accessory proteins.

1.2.2 Transition Zone

There is a conserved structure at the base of axoneme and distal basal body called transition zone (TZ), which acts as a diffusion barrier. Although there are Y-shaped proteins that link microtubules to membrane at TZ in lower organisms, these Y-shaped structures are less obvious in mammalian cells, in which case called ciliary necklace [8]. TZ has also other structures, such as transitional fibers (TF), which anchor basal body to ciliary membrane. There are many ciliary proteins specifically localized at the TZ, such as MKS1, MKS2, NPHP1, NPHP2 and CC2D2A. Although some proteins like CEP290, whose localization is associated with Y-links, function as gate keeper by preventing entrance of non-ciliary proteins; other TZ proteins such as CC2D2A help with the entrance of ciliary proteins by acting on vesicle trafficking [9], [10]. Although many non-ciliary proteins are excluded from cilia by TZ proteins, some non-ciliary proteins fused

to ciliary targeting sequence of SSTR3 are localized to cilia by TZ proteins ARL6 and BBS4 [11]. Proteins localized to TZ also controls the exit of proteins from cilia.

1.2.3 Distal Region

The region which is distal to TZ has different structure and function in different cell types of various organisms [12]. In most of the organisms, distal part of the cilia tends to narrow down towards the tip of the cilia. Microtubule arrangement also changes from doublets to singlet towards the ciliary tip [12], [13]. Although radial organization of microtubules are still preserved towards the distal end of the cilia, the radial shape of microtubules are lost when all doublets become singlets at the tip of the cilia, except a couple of ciliated organisms such as *Chlamydomonas*, which still preserves the central pair [13].

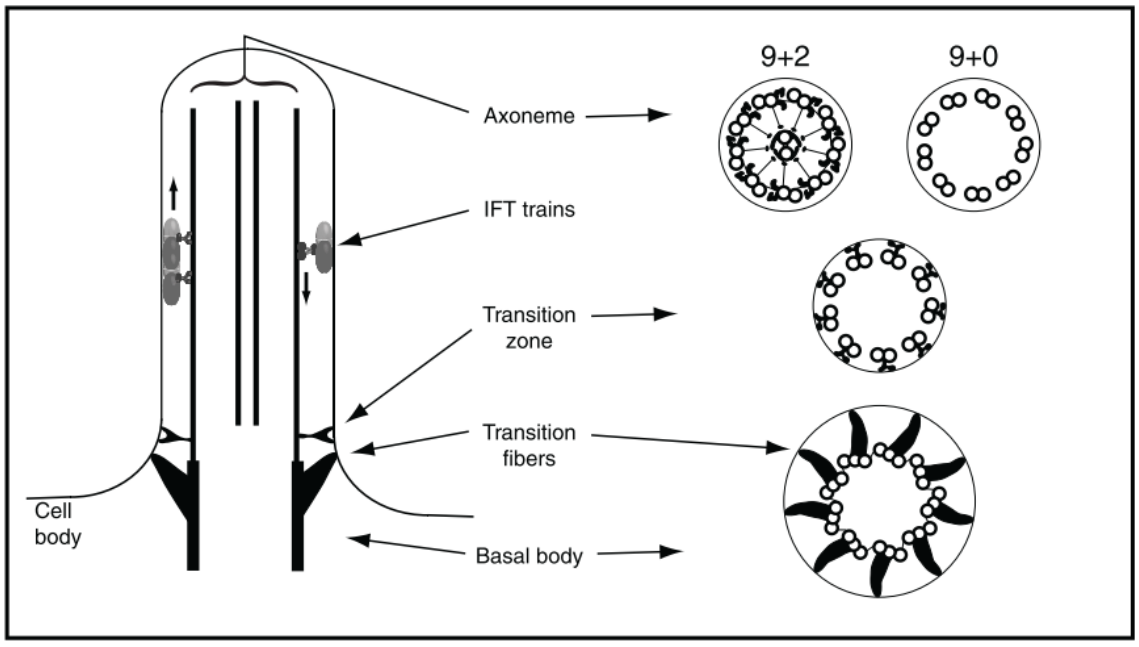

Figure 1.2.1 General structure of cilium.

Cilia are microtubule-based organelles found on majority of mammalian cell types. Ciliary axoneme is surrounded by a membrane, which links to axoneme by transition fibers. While motile cilia are consisting of 9+0 microtubule doublets, non-motile cilia have 9+2 doublets. Figure adapted from Witman *et al.*, 2014.

1.3 The Cilia in *Caenorhabditis elegans*

Caenorhabditis elegans is a nematode that lives everywhere in soil. Because of its short life span, small size, transparency and easiness of genetic engineering, it is used as a model organism. Having 60 ciliated neurons in the 302 neurons total, *C. elegans* exhibits many kinds of sensory behaviors such as odor response, temperature and touch [14], [15]. Despite the very low frequency of producing male (<0,2%), *C. elegans* is mostly self-fertilizing hermaphrodite. It has a rapid life cycle consisting of 6 stages, which are L1, L2, L3, L4, adult and dauer, the latter being a stage L2 worms molt into when they are starved and crowded (Figure 1.3.1) [16]. They can live several months in dauer stage, making maintenance of them easy [17].

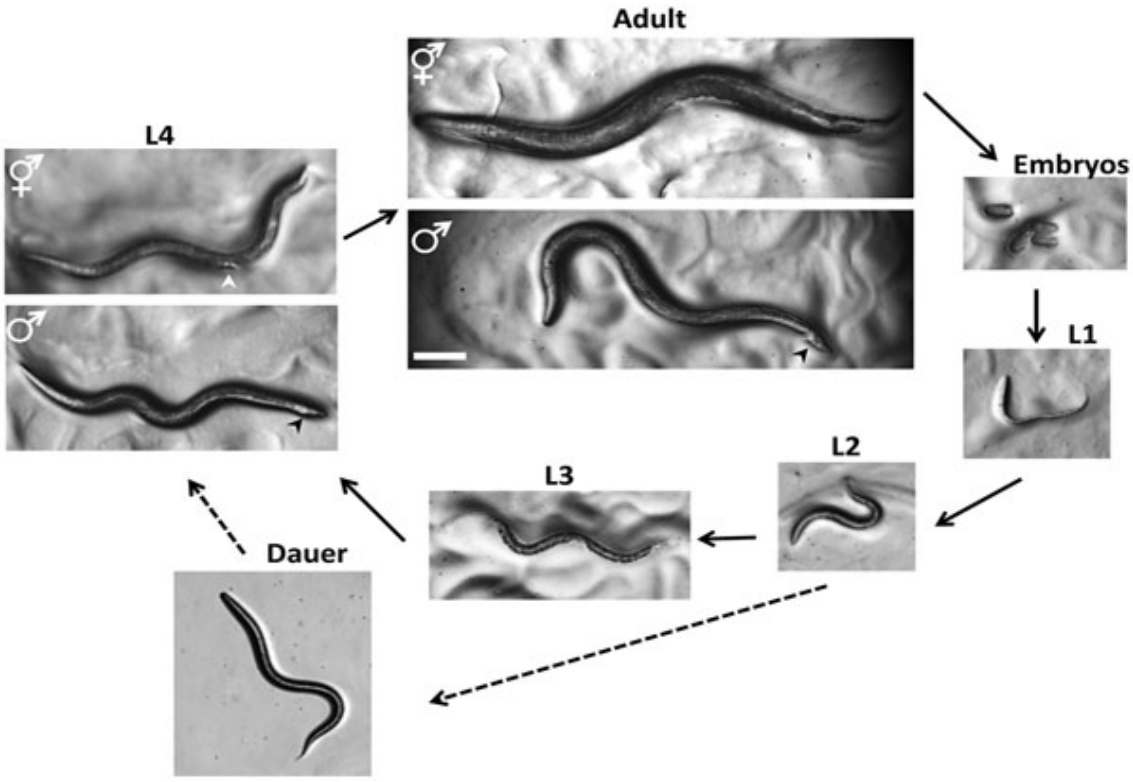

Figure 1.3.1 Life cycle of *C. elegans*.

Shown are nomarski differential interference contrast (DIC) images of *C. elegans*. *C. elegans* are animals that lay eggs, and grow to reach adulthood through four larval stages (L1, L2, L3 and L4). In case of harsh conditions, *C. elegans* enters the dauer stage where worms can live for several months. *C. elegans* has males (XO) and hermaphrodites (XX), with 1031 cells and 959 somatic cells, respectively. The tails of males are different from those of hermaphrodites. Figure adapted from Corsi et al., 2015.

Sensory neurons of *C. elegans* are the only ciliated cells in *C. elegans*. Amphid neurons form the main chemosensory organ of *C. elegans*. The cell body of these neurons is located in anterior part of pharyngeal bulb and have dendrites extends towards anterior part of the *C. elegans* and have cilia with various shapes at the end of the dendrites [14]. Although most of these cilia have single rod or double rod shape (ASK, ASI, ASJ, ASE, ADF, ADL, ASH, ASG), some of the amphid neurons have unusual wing like shape (AWA, AWB, AWC) and some of them are surrounded by microvilli (AFD). AFD and AWA, AWB, AWC neurons are not exposed to outside of *C. elegans*, whereas phasmid cilia (PHA and PHB), which are located in posterior to the anus and other amphid cilia are exposed to external environment [14].

Unlike cilia of mammalian cells, nonmotile cilia of *C. elegans* do not have basal body [14]. Transition zone also differs structurally, as in *C. elegans* it consists of doublet microtubules whereas cilia in other organisms possess triplet microtubules which are considered as basal bodies [14]. Unlike cilia in other organisms, microtubules are arranged as doublets in middle segment and as singlets in distal segment [12].

1.4 Intraflagellar Transport System

Since the cilia lack protein synthesis machinery, the proteins required for biogenesis of cilia and intercellular signaling are not synthesized in cilia. Thus, they must be transported into cilia after being synthesized in the cell [4]. The specialized, bidirectional motility process used to transport ciliary proteins from the ciliary base to the tip of the cilia and from tip to the ciliary base is called intraflagellar transport (IFT). Joe Rosenbaum and his colleges first discovered the bi-directional motility called IFT in 1993 along with the flagella of *Chlamydomonas reinhardtii* when they used differential interference contrast (DIC) microscopy to monitor the flagella [18]. TEM analysis revealed that IFT is positioned between ciliary membrane and doublet microtubules [18]. The same group later biochemically identified the IFT complex containing 15 polypeptides that sub-grouped into two complex IFT-A and IFT-B. The IFT-A subcomplex consists of IFT139,

IFT43, IFT121, IFT140, IFT122 and IFT144, while IFT57, IFT20, IFT46, IFT52, IFT72, IFT74, IFT27, IFT80, IFT81, IFT88, and IFT172 are arranged into the IFT-B subcomplex. The later analysis discovered novel IFT components and Bardet-Biedl Syndrome (BBS) genes that translocate together with IFT complex.

Non membrane bound IFT particles move along the axoneme until tip of the cilia, where they change the direction and start moving towards the base of the cilia. The movement of IFT particles in anterograde direction (from the base to the tip of the cilia) is mediated by Kinesin II motor. On the other hand, the movement of IFT from ciliary tip to base of the cilia called retrograde direction (from the tip of cilia back to the base of cilia) is achieved by cytoplasmic dynein [19]. The later years witnessed that IFT movement occurs in many organisms including *C. elegans* and mammals, and functional analysis of each components revealed that IFT is required for cilia assembly in every organism investigated, suggesting that the cilia assembly relies on evolutionary conserved mechanisms. [19], [20]. It is noteworthy that unlike *C. reinhardtii,* where Kinesin-II is the main anterograde driving motor, *C. elegans* has one additional anterograde kinesin motor OSM-3 (human KIF17) that cooperatively carries IFT particles and ciliary proteins together with Kinesin-II [14].

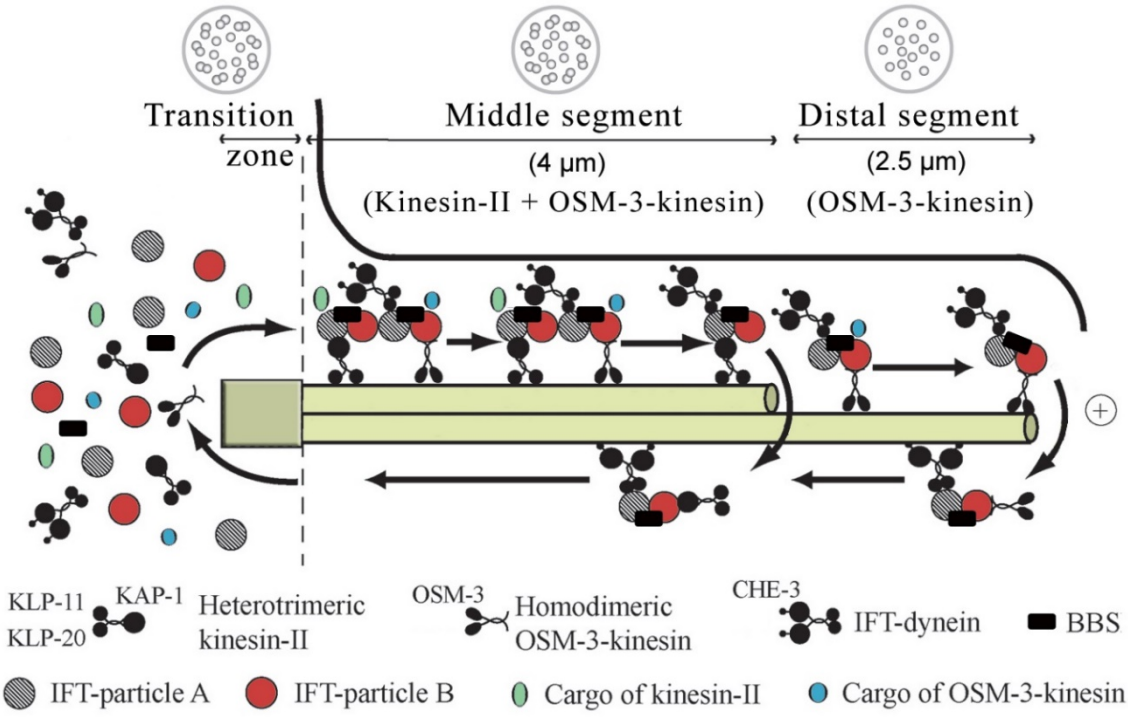

Figure 1.4.1 Intraflagellar Transport system in *C. elegans*

In *C. elegans*, cilia have microtubule doublets in the middle segment while the distal cilia segment possesses a singlet microtubule. OSM-3/KIF17 and heterotrimeric kinesin-II jointly transport the IFT particles along the middle segment with speed of 0.7 μm/s in the anterograde direction, while IFT in the distal segment is powered by OSM-3/KIF17 with a speed of 1.2 μm/s alone. Cytoplasmic dynein mediates the retrograde movement at a velocity of 1.1 μm/s. Figure adapted from Inglis *et al.*, 2007.

1.5 Ciliopathies

Given the importance of cilia in various cellular processes like signal transduction and motility, it is not surprising that many human diseases are related to cilia [1]. The human disorders caused by defects in structure and function of cilia are collectively called ciliopathies [1]. Since cilia are found in a variety of tissue and organ systems, these disorders have diverse phenotypes ranging from cystic kidneys and mental retardation to obesity and retinal degradation (Figure 1.5.1) [21]. Ciliopathies are, most of the time, caused by mutations in evolutionarily conserved genes encoding proteins which are either involved in ciliogenesis or interact with ciliary proteins [21].

1.5.1 Primary Ciliary Dyskinesia

Primary ciliary dyskinesia (PCD) is a ciliary disorder caused by defects in motile cilia. Patients having PCD show sinusitis and chronic bronchitis due to the failure of clearing bacteria and mucus by the motile cilia on the respiratory track [4]. Since the source of ciliary impairment is genetic, other motile cilia are also affected and cannot function, such as male PCD patients are infertile due to the defects in sperm flagellum and some patients' organs have reversed positions due to the impaired right-left asymmetry caused by defects in motility of nodal cilia [4], [22].

1.5.2 Polycystic Kidney Diseases

The role of nonmotile cilia in autosomal dominant polycystic kidney disease (ADPKD) is first shown in C. elegans, which have ortholog of ADPKD associated human polycystin-1 gene expressed in ciliated neurons [4], [23]. Autosomal dominant PKD

results from mutations in genes PKD1 and PKD2, whose encoded proteins function in renal tube differentiation by forming a receptor channel complex through interacting with each other [4], [23]. The disease is often characterized by cyst formation in kidneys [1].

1.5.3 Sensory Ciliopathies

Defects in the sensory and signaling functions of cilia result in sensory ciliopathies. Those sensory and signaling functions are mainly present in non-motile cilia and the ciliopathies associated with disruption of these functions have different phenotypic presentations than PCD [3]. Sensory ciliopathies have various possible causes including defects in ciliary signal transduction pathway components, impaired cilia formation and trafficking defects [3].

Sensory ciliopathies like retinal degeneration and anosmia are thought to be the result of defects in opsins and olfactory receptors mediated ciliary signaling [24], [25]. In retinal degeneration, for example, cilium length control and formation are impaired and ciliary cGMP concentration mediating enzyme is disrupted. In these cases, apoptotic cell death is promoted by the ciliary defects via a mechanism involving accumulation of opsin in the ER, resulting in unfolded protein response (UPR) [26].

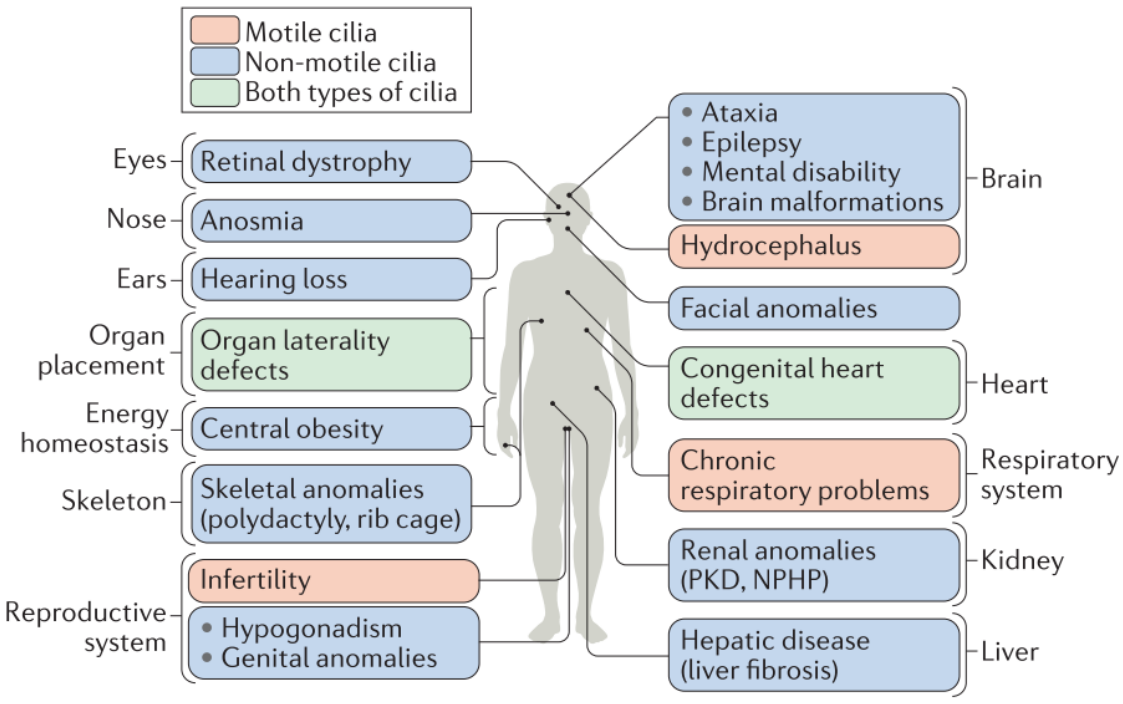

Figure 1.5.1 Defects in cilia cause a wide range of diseases called ciliopathies

Defects in cilia structure and/or cilia function result in a range of diseases called ciliopathies, signifying the importance of cilia function for each organ. Ciliopathies are multi-organ diseases which can affect almost all parts of the human body. Both motile and non-motile cilia are associated with ciliopathies. Figure adopted from Reiter *et al*., 2017

1.6 G protein-Coupled Receptors (GPCR)

GPCRs are the largest family of signaling receptors and membrane proteins which mediate vision, taste and olfaction by responding to external signals, mediating responses of the cells to neurotransmitters and hormones and mediating associated signaling pathways [27], [28]. Therefore, many therapeutic drugs target GPCRs as they are common in most of the signaling pathways. Although they have functional variety, all GPCRs have seven transmembrane domains, carboxyl terminus at intracellular part and an amino terminus in extracellular part of the protein [28].

Since there are many GPCRs and their effector molecules are enriched on the cilia of different cell types, cilia is responsible for various GPCR signaling [28], [29]. Therefore, most of the work about GPCRs are related to ciliary GPCR identification in neuronal cells as primary cilia can be found on most of the mammalian neurons [29]. Although it is difficult to identify new ciliary receptors, new insights on especially ciliary targeting sequences have made it easier to narrow down potential ciliary GPCRs.

Until now, three ciliary targeting motifs (CTS) have been found in third intracellular loop or C terminal tail of GPCRs. These are C-terminal VxPx CTS of rhodopsin, Ax[S/A]xQ domain of IC3 domain in Sstr3 and Htr6, and [R/K][I/L]W motif in IC3 domain of NPY2R [29]. Since these motifs can be seen in ciliary GPCRs, proteins containing these motifs might be considered as ciliary GPCR and further analysis can be performed.

1.7 CRISPR/Cas9

Being able to edit DNA of genome has tremendous value for functional studies of genes and genetic diseases. There have been many tools that can introduce changes into genomes like ZNFs and TALEN, which are effective but not cost efficient. The studies showing that exogenous DNA can be inserted into the genome through homologous recombination in mammalian cells have led many researchers work on DNA editing systems [30], [31]. However, due to the limitations of this approach such as low copy of spontaneously integrated DNA and undesirable results due to random integration of exogenous DNA into various parts of the genome; alternative approaches were sought to overcome these limitations [31].

After finding that double stranded breaks (DSB) increase integration of exogenous DNA into the genome, researches began focusing on strategies to introduce DSBs to specific target DNAs [31]. To this end, researchers began to engineer nucleases such as meganucleases, zinc-finger nucleases (ZFNs) and transcription activator-like effector nucleases (TALENs) [32]. Each of these protein-based systems have their own advantages and disadvantages. In 2013, Feng Zhang and colleagues has engineered CRISPR/Cas system to introduce precise cleavage into genome of mouse and human cells [33]. CRISPR (Clustered regularly interspaced short palindromic repeat DNA sequences) is first found in E. coli in 1987 by Dr. Nakata and his colleagues [34]. Later, it was found that bacteria integrate new spacers from genomic sequences of infecting phage by using CRISPR and associated cas enzymes as a defense mechanism [35]. The integrated spacer sequences are transcribed (crRNA) and incorporated with transactivating CRISPR RNA (tracrRNA). The resulting RNA sequence (sgRNA) forms a complex with Cas9, which is a nuclease expressed in *Streptococcus pyogenes*; and the complex then cleave target DNA sequences which is complementary to the integrated spacer sequences (Figure 1.7.1a) [32], [36].

This defense mechanism of bacteria against phages are utilized to achieve targeted precise genome editing in CRISPR/Cas system, in which a guide RNA (gRNA) and Cas9 nuclease are introduced in the cell [32]. The Cas9 can be utilized directly as enzyme, as well as can be introduced in a plasmid. crRNA part of the gRNA, which lies at the 5' end

of gRNA, consists of 20 nucleotides and can direct Cas9 to the specific target site on DNA, which must be 5' end of a PAM sequence (Figure 1.7.1a). Two of the most used PAM sequences are 5'-NGG and 5'-NAG. This feature of crRNA is used to target any site which is 5' end of a PAM sequence.

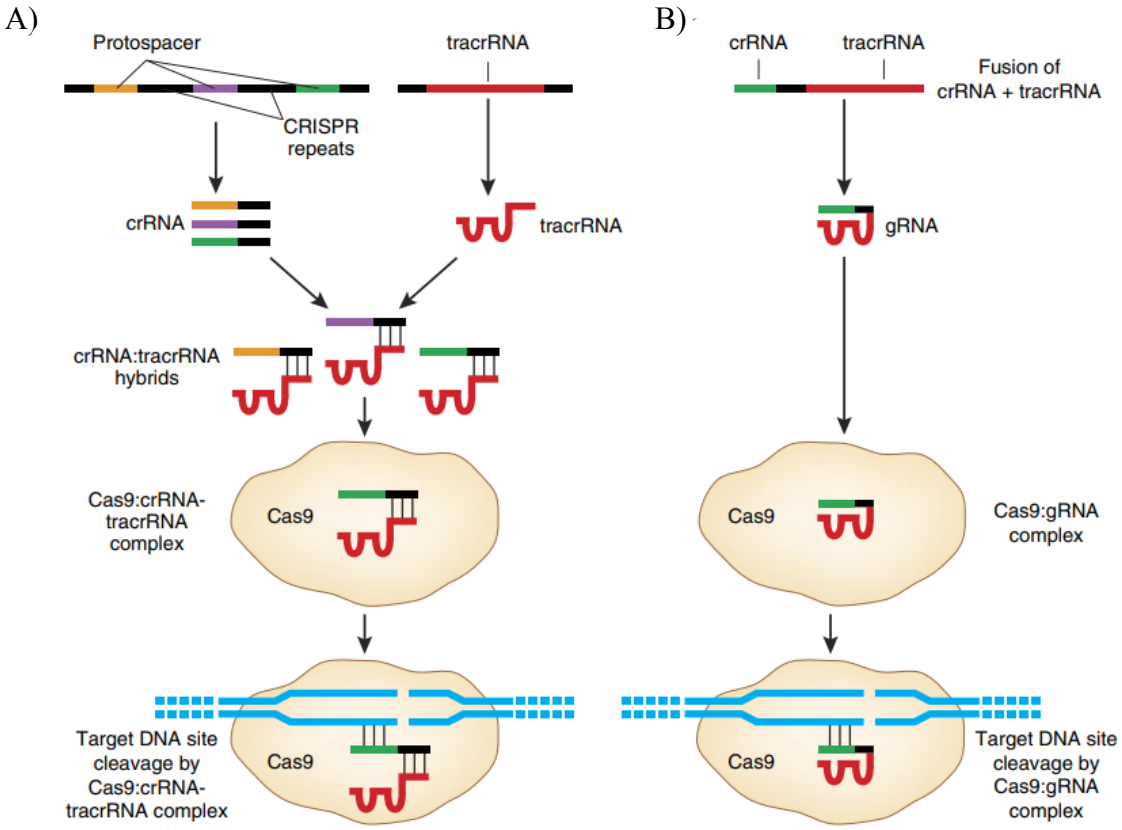

Figure 1.7.1 CRISPR/Cas systems

(A) Natural CRISPR/Cas mechanism found in bacteria as a defense mechanism. (B) CRISPR/Cas9 system which is artificially engineered for precise genome editing. Figure adopted from Sander *et al.*, 2014

Chapter 2

Materials and Methods

2.1 Materials

2.1.1 Strains

The strains used in this work:

N2

bbs-5 (gk537)

nphp-4 (tm925)

arl-13 (gk513)

mks-5 (tm3100)

grk-2 (gk268)

cep41 (tur001)

arl-13 (tm2322)

nphp-2(gk653)

N2; Ex [C15A7.2promoter-C15A7.2::GFP +pRF4]

vuaSi21 [pBP39; *Pmks-6*::MKS-6::mCherry; cb-unc-119(+)]II

N2; Ex [MKS-2::GFP +XBX1::tdTOMATO+pRF4]

N2; gmls13 (*srb-6p*::GFP+pRF4)

N2; [Pstr1promoter::GFP]

kyIs141 [OSM-9::GFP5 + lin-15(+)]

N2; Is [OSM6::GFP]

him-5 (e1490); myIs1 [PKD-2::GFP + Punc-122::GFP]

oyIs65[*str-1p*::mCherry]

The following strains were generated in this work:

tmem-145 (tur002)

tmem-145 (tur009)

Ex [C15A7.2promoter-C15A7.2::GFP +pRF4]; vuaSi21 [pBP39; Pmks-6::mks-6::mCherry; cb-unc-119(+)]

tmem-145 (tur002); *nphp-4 (tm925)*

tmem-145 (tur002); *bbs-5 (gk537)*

tmem-145 (tur002); Ex [MKS-2::GFP +XBX1::tdTOMATO+pRF4]

tmem-145 (tur002); gmls13 (*srb-6p*::GFP+pRF4)

arl-13 (gk513); gmls13 (*srb-6p*::GFP+pRF4)

nphp-4 (tm925); gmls13 (*srb-6p*::GFP+pRF4)

mks-5 (tm3100); gmls13 (*srb-6p*::GFP+pRF4)

tmem-145 (tur002); *arl-13 (gk513)*; gmls13 (*srb-6p*::GFP+pRF4)

tmem-145 (tur002); *nphp-4 (tm925)*; gmls13 (*srb-6p*::GFP+pRF4)

tmem-145 (tur002); *mks-5 (tm3100)*; gmls13 (*srb-6p*::GFP+pRF4)

tmem-145 (tur002); [P*str1*promoter::GFP]

grk-2 (gk268); [P*str1*promoter::GFP]

tmem-145 (tur002); *grk-2 (gk268)*; [P*str1*promoter::GFP]

tmem-145 (tur002); [osm-9::GFP5 + lin-15(+)]

tmem-145 (tur002); him-5 (e1490)

tmem-145 (tur002); Is [OSM6::GFP]

tmem-145 (tur002); cep41 (tur001); Is [OSM6::GFP]

him-5 (e1490); myIs1 [PKD-2::GFP + Punc-122::GFP]

him-5 (e1490); *tmem-145 (tur002)*; myIs1 [PKD-2::GFP + Punc-122::GFP]

him-5 (e1490); *tmem-145 (tur002)*; *nphp-2(gk653);* myIs1 [PKD-2::GFP + Punc-122::GFP]

him-5 (e1490); *arl-13 (gk513)*; myIs1 [PKD-2::GFP + Punc-122::GFP]

him-5 (e1490); *tmem-145 (tur002)*; *arl-13 (gk513)*; myIs1 [PKD-2::GFP + Punc-122::GFP]

tmem-145 (tur009); oyIs65[*str-1p*::mCherry]

2.1.2 Primers and Plasmids

The following list is the primers and plasmids used in CRISPR/Cas9 gene editing.

C15A7.2_sgRNA1_For: TCTTGCTCAGGGAAAGCGTGCTCA

C15A7.2_sgRNA1_Rev: AAACTGAGCACGCTTTCCCTGAGC

C15A7.2_sgRNA2_For: TCTTGCCTACCGATTATATTGACAT

C15A7.2_sgRNA2_Rev: AAACATGTCAATATAATCGGTAGGC

C15A7.2_sgRNA3_For: TCTTGAATTTGGCGTCTCACAGCGT

C15A7.2_sgRNA3_Rev: AAACACGCTGTGAGACGCCAAATTC

pRB1017 was a gift from Andrew Fire (Addgene plasmid # 59936; http://n2t.net/addgene:59936 ; RRID:Addgene_59936)

The following primers were used in sanger sequencing

C15A7.2_CRISPR_For: gaagcagttcgtgactaccag

C15A7.2_CRISPR_Rev: CCACAATGTTCACCACTTCCG

2.2 Methods

2.2.1 CRISPR/Cas9 Gene Editing

For knock out experiment, three different sgRNAs were designed. An empty vector for sgRNA cloning pRB1017 (Addgene: #59936), harboring CeU6 promoter for *C. elegans* expression, Kanamycin resistance gene for selection and a gRNA scaffold for successful sgRNA integration to Cas9, was used to clone three different sgRNA oligonucleotide pairs (forward and reverse). sgRNAs were designed using SYNTHEGO CRISPR tool (design.synthego.com). The primers with maximum on target and minimum off target scores were selected and a small sequence which is complementary to cut site of the vector were added to 5' and 3' ends of the primers according to the protocol [37]. Primers and their complementary strand primers (forward and reverse) were ordered from Macrogen. Primers were cloned into pRB1017 vector using Golden gate assembly technique. First, forward and reverse primers (1 µl each) were annealed in a mix of 2 µl 10x T4 ligase buffer (Thermo) and 6 µl ddH_2O; and incubated for 5 min at 95ºC, then let to slowly cool until room temperature using Thermo Scientific Thermocycler. Annealed primers were then incubated with 0.5 µl BsaI restriction enzyme, 0.5 µl T4 DNA ligase, 2 µl T4 DNA ligase buffer, 1 ug pRB1017 vector and ddH_2O until a total of 20 µl, for 1 hour at 37ºC, 5 min at 50ºC, and for 20 min. at 65ºC. The ligation product was then chemically transformed into E. coli dh5alpha strain. For transformation, first, *E. coli* were exposed subsequent $CaCl_2$ treatment to induce competency to take up plasmids into the cell. Then, these chemically competent cells were incubated with ligation product for amplification of the plasmid for 20 min on ice. Next, heat shock was induced at 42ºC for 45 sec in water bath. Then after 2 min incubation on ice, cells were incubated at 37ºC for 20 min to express required proteins before plating on agar plates with kanamycin. Then cells were incubated at 37ºC overnight. To confirm that the sgRNAs are successfully

inserted into the vector, colony PCR was performed for selected 5 colonies for each sgRNA. The colonies whose plasmid was amplified were grown in LB broth overnight at 37ºC. Plasmids containing sgRNAs were isolated using TransGen EasyPure Plasmid MiniPrep kit.

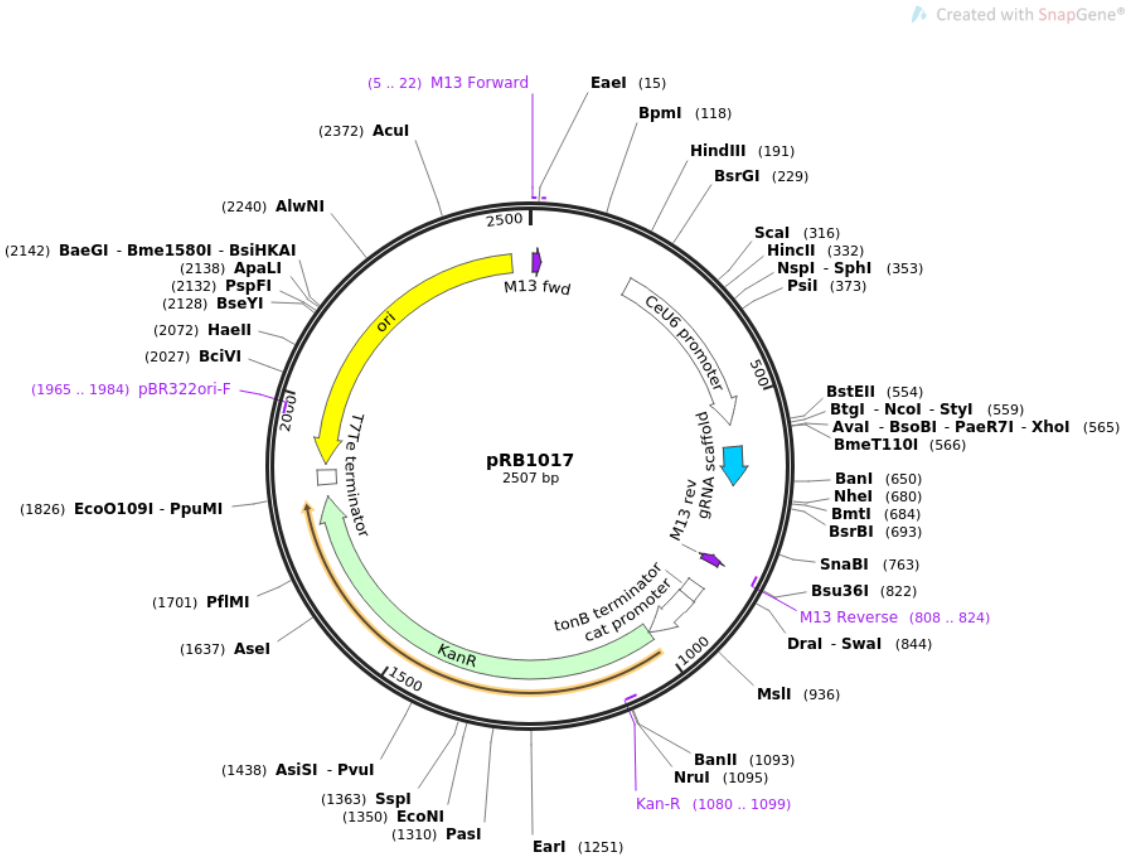

Figure 2.2.1.1 Schematic representation of Prb1017 plasmid

pRB1017 plasmid engineered to be utilized as sgRNA carrier for CRISPR/Cas9 in *C. elegans*. BsaI restriction sites enable one step Golden Gate Assembly of primers to the vector. Figure adapted from plasmid's Addgene page: https://www.addgene.org/59936.

2.2.2 Microinjection in *C. elegans*

For microinjection, an injection mix was prepared. 50 ng of each three sgRNAs (C15A7.2_sgRNA_1, C15A7.2_sgRNA_2 and C15A7.2_sgRNA_3) were mixed with 15

ng pad650(peft::cas9) empty vector and 25 ng pAD67 pRF4 (roller marker). The mixture then was centrifuged at 14000 rpm for 10 min at 4°C.

Injection pad is a platform on which worms were put and immobilized to inject plasmids easily. Injection pads were prepared one day before injection in order to ensure that they are dry enough to keep worms immobile. To prepare pads, 2% agarose in water was boiled and 1-4 drops of boiled agarose solution were put onto the center of a glass coverslip. Another glass coverslip was immediately put on the agarose drop and after a few seconds, it was slowly slide off. The pads on slides were let dry for one day.

C. elegans microinjection requires a very thin, glass needles in order to inject plasmids into gonad without damaging the worms. For that, needle tips were prepared by using a heater. First, the temperature was set to 65°C and 60°C on heater to make sure that needles are sharp enough to penetrate into worms easily. Then the capillary glass was inserted into ridges and both top and bottom knobs were tightened. Device was then started and two needles were generated.

In order to load the needle with injection mix, 1 µl mix was first taken up with a syringe, then loaded into the needle from broad end of needle. Back end of the needle was attached to N_2 gas tube. The needle then was attached to needle holder by first unscrewing the holder and after inserting the needle screwing the holder back. The needle was arranged so that the tip makes 45° angle with stage. The balance is set to ON and the balance value was set to 120 mpa. The pressure was set to 200 mpa. It is important to set balance to a value so that the mix inside the needle should be in the middle of the capillary tube. This was generally achieved when the balance set to 120 mpa.

To prepare worms for injection, wild type worms which are in L4 stage were put on an agar plate one day before injection as young adult worms are required for a successful injection. In the day of injection, a drop of halocarbon oil was put on injection pad. Then 5-6 worms were transferred to an empty agar plate (without bacteria) to avoid transferring bacteria to injection pad. Then these worms were put in oil and wait until they stop moving. Worms then were arranged vertically for easier injection. Needle was positioned to make 15° to 45° degree with the worms and brought into the same level with worms. Focus was changed to show the syncytial gonad arm and worms were gently moved towards the needle and the needle was penetrated into gonad. After injecting the mix, needle was removed gently by moving the platform in reverse direction. After all worms were

injected, recovery buffer was poured on worms and worms were picked up and transferred to a new agar plate. After 1-2 hours of injection, all collected worms were singled out to different plates.

2.2.3 Worm Maintenance and Strains

NGM agar plates were prepared by mixing 2.1 gr NaCl, 1.75 gr bactopeptone, 11.9 gr Agar-agar in 682.5 ml dH_2O and the mixture was autoclaved at 121°C. After the autoclave, bottle was left cooling until the temperature of the bottle becomes 45°C. Then 700 µl cholesterol, 700 µl nystatin, 12.5 ml KH_2PO_4, 700 µl $CaCl_2$ and 700 µl $MgSO_4$ were added into liquid agar and poured into petri dishes. After letting it cool at room temperature overnight, 150 µl of OP50 strain of *E. coli* bacteria which was grown in LB overnight at 37°C was put on agar plates and spread using a spreader.

All worms were maintained on NGM agar plates with spread OP50 E. coli strain at 15°C and 20°C. Young adult worms were used for microscopic analysis. For dye filling assay, worms from various stages were incubated in dye solution (dye was diluted in ratio of 1:1000 in M9 buffer) for 45 min in a dark environment. Then worms were washed with M9 and put on NGM agar plates. Worms were analyzed with compound microscope with red fluorescent light.

2.2.4 Microscopic Analysis

For microscopic analysis, slides were coated with 2% agarose and one drop 25 µM levamisole was added onto agarose jel. Adult worms were put in levamisole on slides and a cover slide was put on the slides. Most analysis were performed at 20°C using Leica DM6 B fluorescent microscopy and images were taken with Andor iXon Ultra camera using Andor iQ 3.6.2 software, under 20x and 100x magnification. Some analysis were performed using ZEISS LSM 900 confocal microscopy using ZEISS ZEN 3.0 (blue edition) software. Analysis were performed using ImageJ2 software. IFT speeds were measured by generating kymographs and measuring the slope of the lines using ImageJ2 software. Since all values are in pixel, they were then multiplied by pixel size and fps to find the actual speed in µm/s. Cilia lengths were measured by ImageJ2 using “measure”

feature. Fluorescence intensity was measured by drawing a shape in the most intense areas of both cell body and cilia, then drawing the same shape in an area with the least fluorescence intensity for measuring background noise. Background intensity was subtracted and calculated the ratio of cilia/cell body fluorescent intensity.

Chapter 3

Results

3.1 *C15A7.2* Is The Homolog of Human *TMEM145* Gene

Before I joined the lab, the Kaplan lab used single cell RNA sequence (scRNA) approach to compare the gene expression profiles of ciliated cells with those of non-ciliated cells to identify novel ciliary gene candidate. Among putative ciliary candidate genes, I have started to characterize the role of uncharacterized conserved gene *C15A7.2* (Human TMEM145*).* We first performed reciprocal Blast analysis for *C15A7.2* and showed that *C15A7.2* is indeed homologous to human *TMEM145* with 83% coverage and 32.8% identity to human TMEM145 (Fig. 3.1.1A). Similar to human TMEM145, *C. elegans* TMEM-145 contain a rhodopsin-like GPCR transmembrane domain, further strengthening the notion that *C. elegans C15A7.2* is orthologous to human TMEM145 (Figure 3.1.1B). Therefore, we rename *C. elegans C15A7.2* gene as *tmem-145*.

According to scRNA-seq analysis, *tmem-145* expressed exclusively in ciliated sensory neurons in *C. elegans.* We first generated transgenic *Ex[C15A7.2promoter::GFP +pRF4]* strain in *C. elegans* to confirm the expression of *C15A7.2* in ciliated cells. Our microscopy analysis confirmed that *tmem-145* is only expressed in the ciliated sensory neurons in *C. elegans*, suggesting that tmem-145 might be involved in cilia biogenesis.

A)

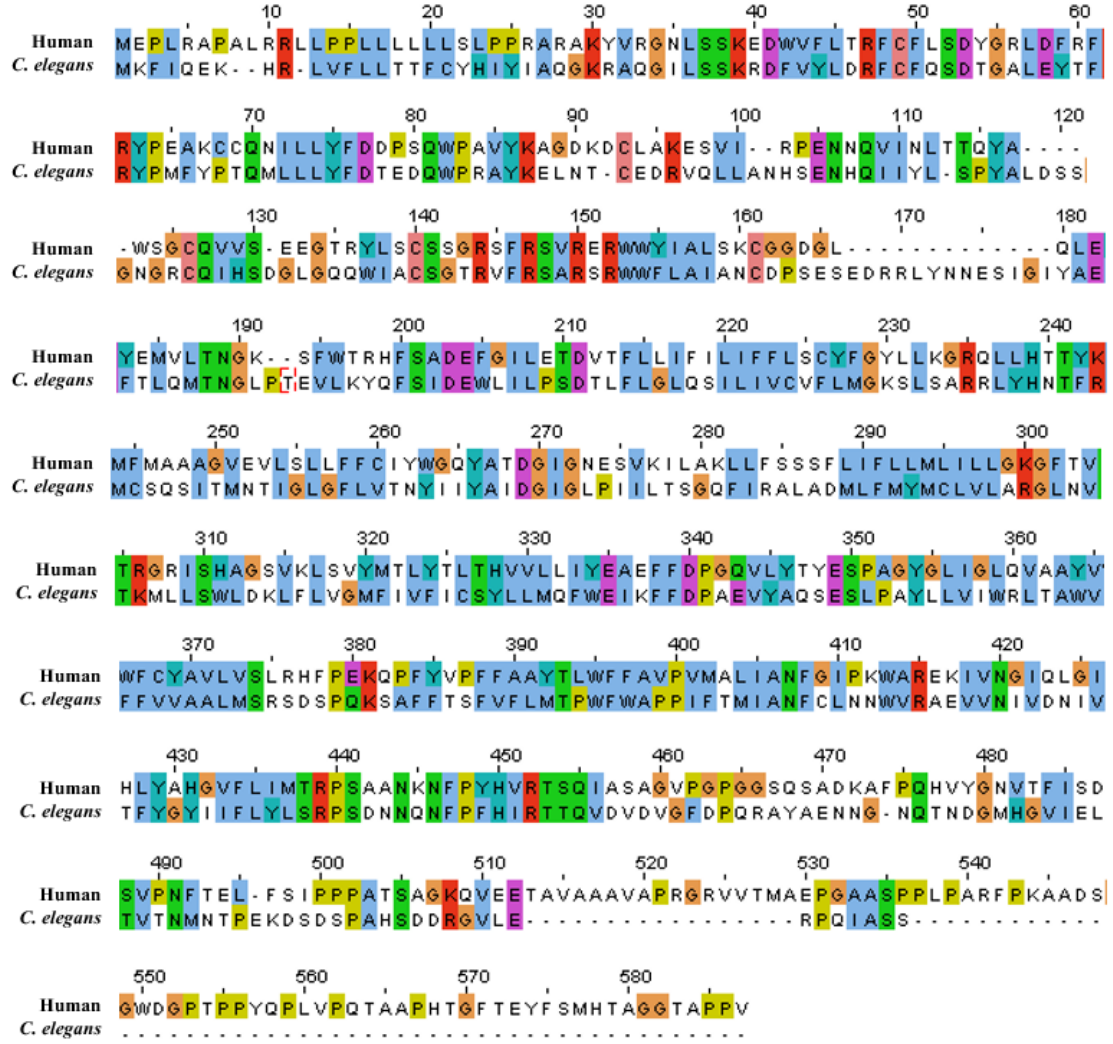

B)

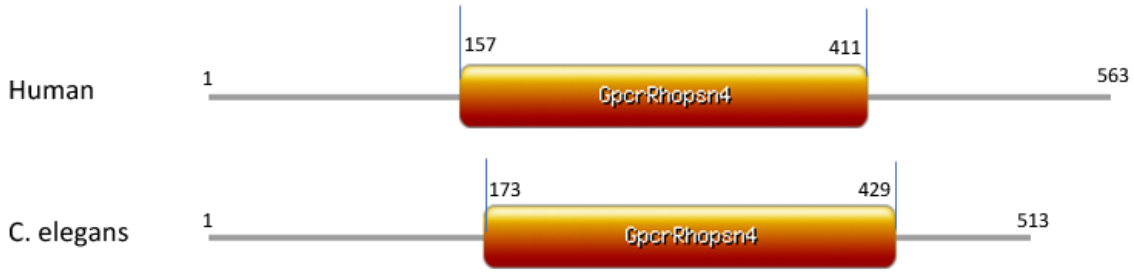

Figure 3.1.1 *C15A7.2* is the homolog of human *TMEM145* gene

(A) Blast analysis showing that *C15A7.2* has 32.8% identity and 83% coverage with human TMEM145 gene. (B) Representation of *C. elegans* and human *TMEM145* genes indicating the GpcrRhopsn4 domains and their positions in the gene

3.2 TMEM-145 Localizes Only in Ciliated Cell to Both Head and Tail Cilia

Having established the cilia specific expression of *tmem-145* in *C. elegans*, we tried to determine if *tmem-145* localizes specifically to cilia. We have generated TMEM-145::GFP; MKS-6::mCherry strain by first constructing TMEM-145::GFP containing all of the coding sequence with 1159 bp upstream of *tmem-145* as promoter, and injecting it on top of MKS-6::GFP strain. TMEM-145::GFP was observed to be exclusively located to the middle segment of amphid and phasmid cilia (Figure 3.2.1). Analysis on confocal microscopy has shown that localization of TMEM-145::GFP was enriched in the middle segment, excluded from both distal segment and transition zone (Figure 3.2.1).

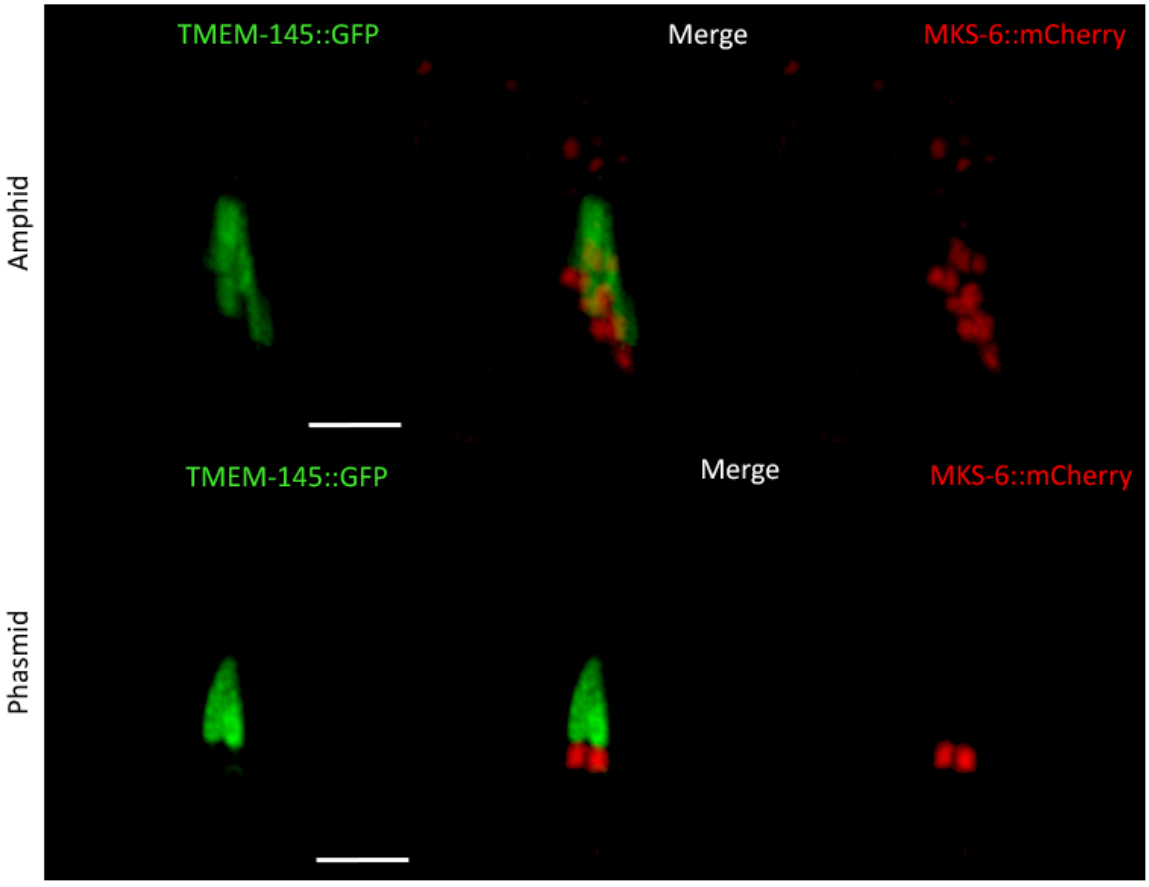

Figure 3.2.1 TMEM-145 localizes to both head and tail cilia

Shown are subcellular co-localizations of TMEM-145::GFP and MKS-6::mCherry in the ciliated sensory neurons in *C. elegans*. The top panel displays the localization of both proteins tagged with fluorescence in the amphid cilia (head) while the bottom panel is phasmid cilia (tail). MKS-6::mCherry specifically localizes to the transition zone (TZ) while TMEM-145::GFP are excluded from the TZ and is localized at

the both amphid and phasmid cilia. The merged confocal images are shown in the middle. Scale bars, 5 µm.

3.3 TMEM-145 Is Not Necessary for Ciliogenesis

Since it localizes to middle segment of cilia, we sought if any ciliary defects occur when the function of *tmem-145* was disrupted. We have generated *tmem-145(tur002)* mutant worms, lacking half of the first exon and second, third and forth exons, as well as a small part of the fifth exon (Figure 3.3.1). To test the effect of *tmem-145* mutation on cilia integrity, we have generated multiple transgenic alleles with *tmem-145(tur002)* mutation.

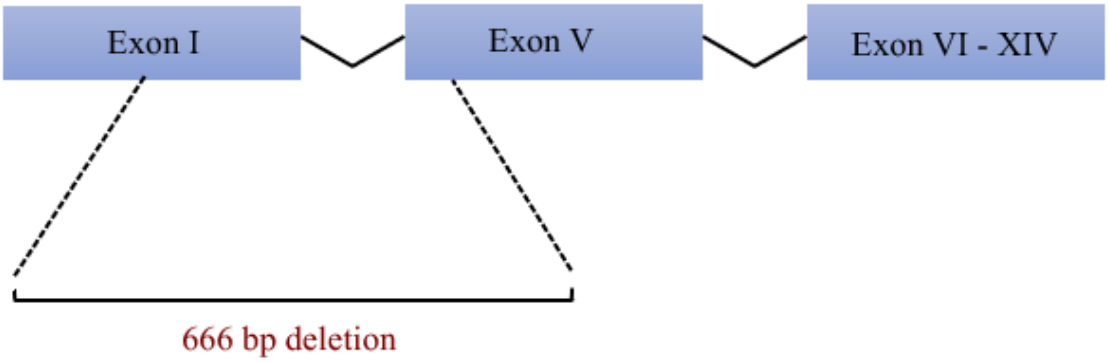

Figure 3.3.1 *tmem-145(tur002)* allele has 666 bp deletion.

Gene model of *tmem-145(tur002)* allele having 666 bp deletion covering half of exon I and 15 bp of exon 5.

In wild type worms, the exposed cilia of phasmid (PHA/B) and amphid neurons take up fluorescent dyes like Dil when the worms are exposed to this dye [38]. If the neurons are not filled with dye, this generally means that the cilia are defective and the worms are called Dyf (Dye-filling defective) [39]. To test if the cilia is defective, we have performed dyf essay and *tmem-145(tur002)* mutants exhibit same dye filling with wild type (Figure 3.3.2).

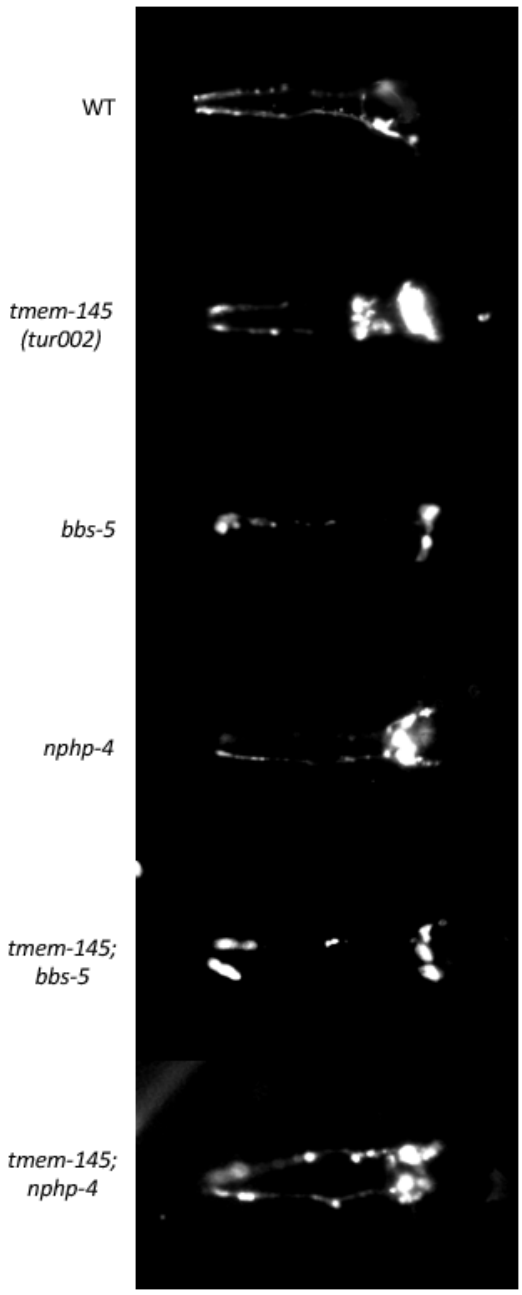

Figure 3.3.2 Function of cilia in *tmem-145(tur002)* mutants are not defective.

Representative images of amphid cilia and cell bodies in WT and *tmem-145(tur002), bbs-5, nphp-4, tmem-145(tur002);bbs-5 and tmem-145(tur002);nphp-4* mutant worms after dye filling assay are shown. All worms uptake the dye.

Next, we have examined the localization of transition zone protein MKS-2 in *tmem-145(tur002)* mutant to see if transition zone is still functioning in *tmem-145(tur002)* mutant worms. We have generated *tmem-145(tur002)*;[MKS-2::GFP;XBX-1::tdTomato] transgenic strain. Transition zone was still intact in *tmem-145(tur002)* mutants and the

localization of MKS-2::GFP was the same in *tmem-145(tur002)* mutant with wild type (Figure 3.3.3).

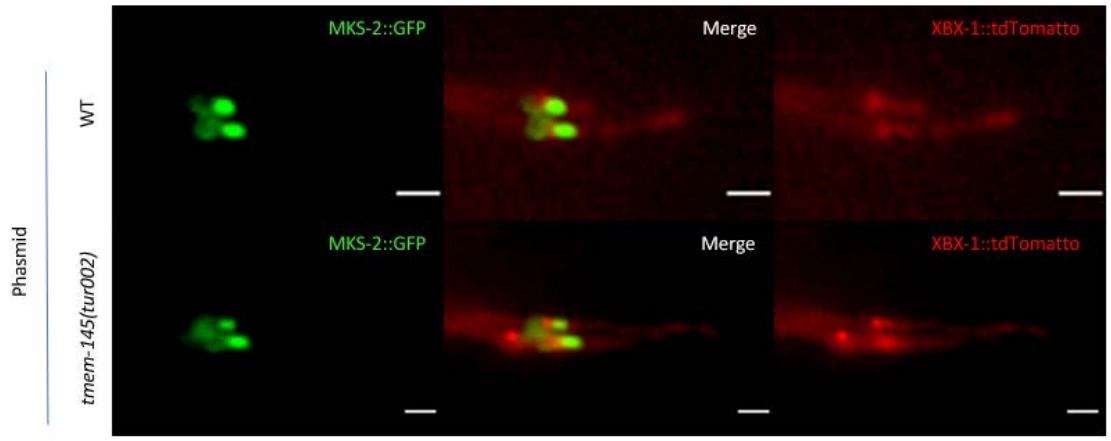

Figure 3.3.3 Localization of transition zone protein MKS-2 is not affected in *tmem-145(tur002)* mutants

Shown are representative images of MKS-2::GFP (human TMEM256) and XBX-1::tdTomato (Human DYNC2LI1) in the tail of wild type (WT) and tmem-145(tur002) mutants. MKS-2::GFP and XBX-1::tdTomato images are displayed on the left and right, while merge images are displayed in the middle, respectively. MKS-2::GFP marks the transition zone while XBX-1::tdTomato stains the entire cilia. Microscopy images show none of these markers are affected in *tmem-145(tur002)* mutants.

Then, we have expressed *srb-6p*::gfp in *tmem-145(tur002)* mutant to visualize the morphology of cilia in *tmem-145(tur002)* mutant. The structure of PHA/B cilia in *tmem-145(tur002)* mutants were the same with the cilia of wild type worms, (Figure 3.3.3). We have then generated *tmem-145(tur002);[str-1p::gfp]* strain to look at the structure of AWB cilia in *tmem-145(tur002)* mutants. No gross abnormal cilia structures were observed in *tmem-145(tur002)* mutants (Figure 3.3.4). We have then investigated cilia structure in OLQ neurons by using OSM-9::GFP that labels OLQ cilia. In both *tmem-145(tur002)* mutant and wild type worms the same OLQ cilia structure was observed (Figure 3.3.5). Taken together with Dye assay findings, all these data suggest that *tmem-145* is required for the ciliogenesis in *C. elegans.*

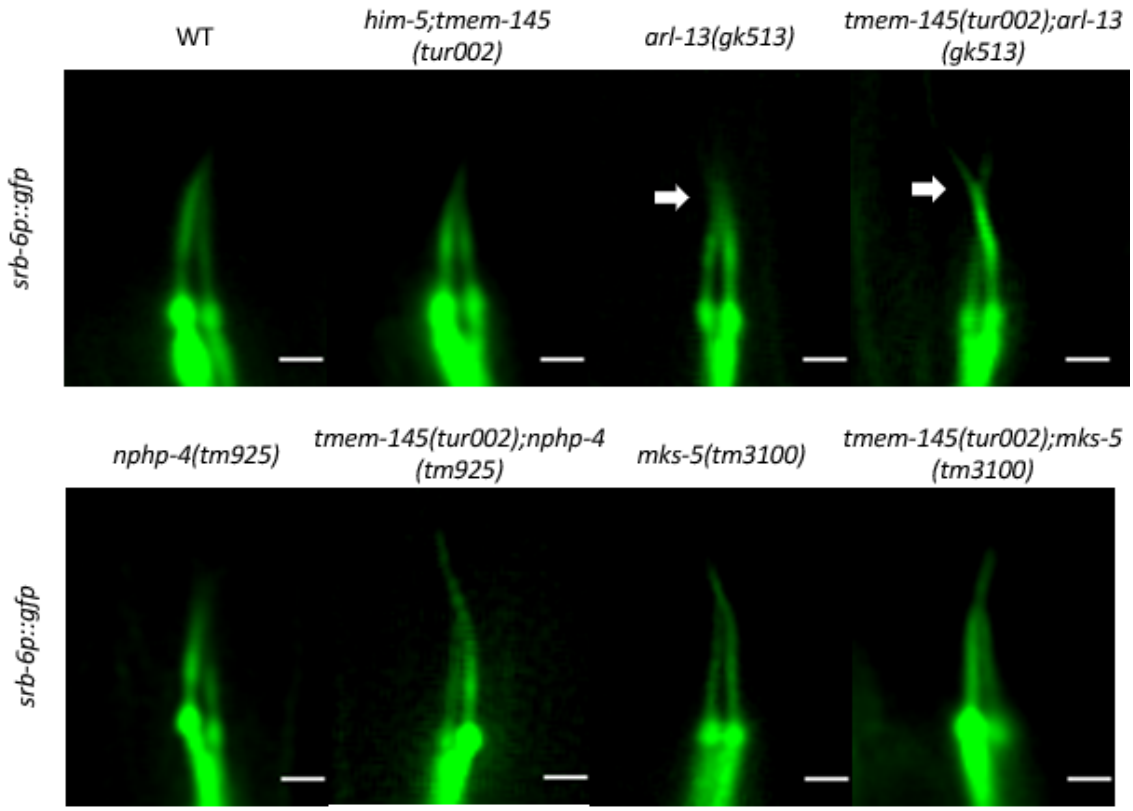

Figure 3.3.4 *tmem-145(tur002)* mutation has no effect on PHA/B cilia structure and has no additive effect on ciliary defects in *arl-13* mutants.

Fluorescent images of PHA/B cilia in wild type, single *tmem-145(tur002)*, *arl-13, nphp-4, mks-5;* as well as double *tmem-145(tur002);arl-13, tmem-145;nphp-4,* and *tmem-145(tur002);mks-5* mutants expressing transcriptional GFP marker *srb-6::gfp* are shown. Arrows indicate kinky PHA/B cilia. Scale bars are 2 μm.

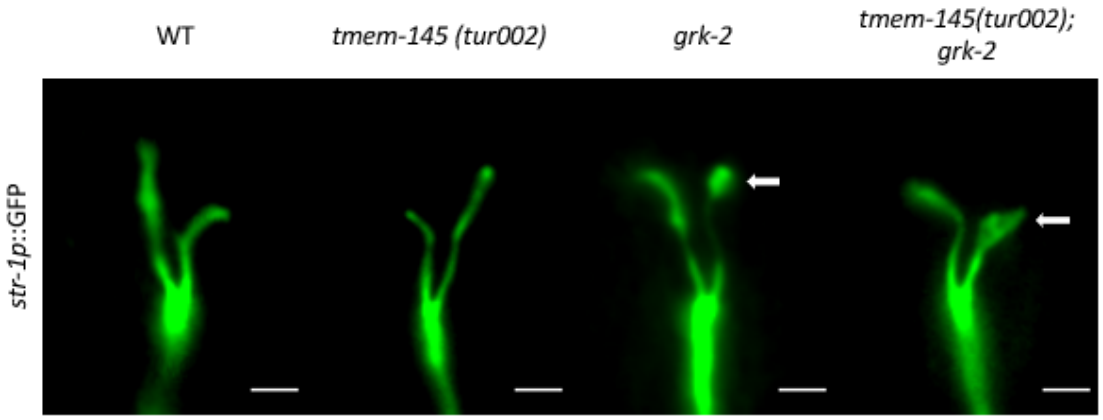

Figure 3.3.5 *tmem-145(tur002) mutation in C. elegans* does not rescue fan phenotype in AWB cilia of *grk-2* mutants.

Representative images of AWB cilia of wild type, *tmem-145(tur002)* single, *grk-2* single and *tmem-145(tur002); grk-2* double mutant worms are shown. Arrows indicate fan-like shape of AWB cilia. Scale bars are 2 μm.

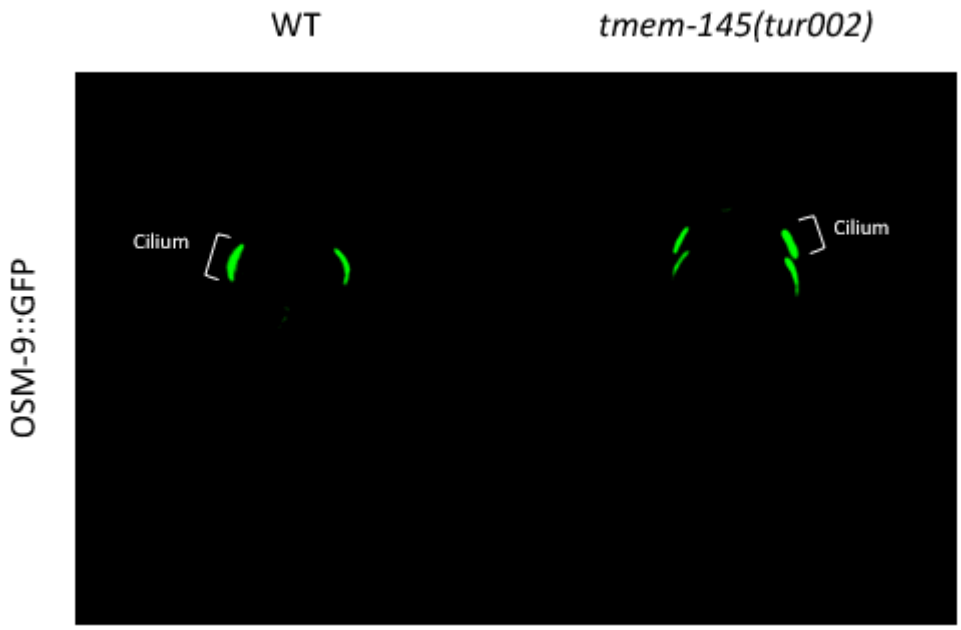

Figure 3.3.6 OLQ cilia have the same structure in *tmem-145(tur002)* mutants with wild type

Representative images of OLQ cilia of wild type and *tmem-145(tur002)* mutant worms are shown. The structure of OLQ cilia is monitored with OSM-9::GFP (a transmembrane protein).

To investigate both localization and speed of IFT protein in *tmem-145(tur002)* mutants, we have generated *tmem-145(tur002);*[OSM-6::GFP] transgenic strain. Although the localization of OSM-6 was the same in *tmem-145(tur002)* with wild type; IFT speed in middle segment of phasmid cilia was significantly lower in *tmem-145(tur002)* mutant than wild type (Figure 10C). Cilia length was the same with wild type (Figure 10B).

A)

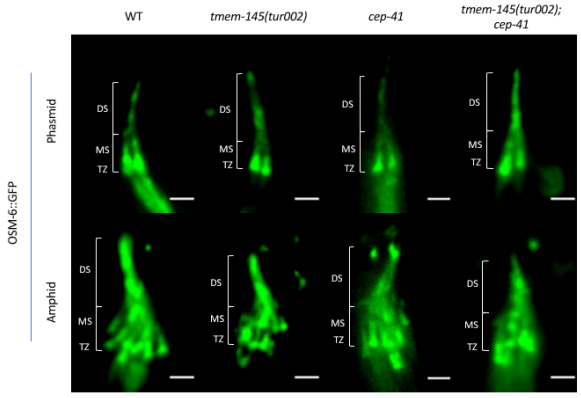

D)

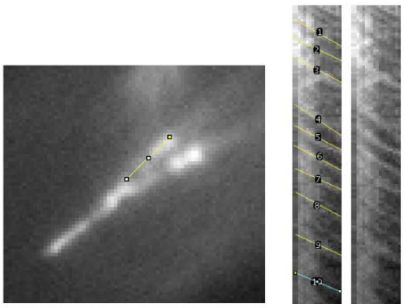

B)

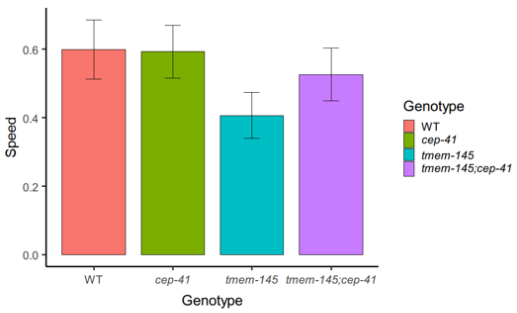

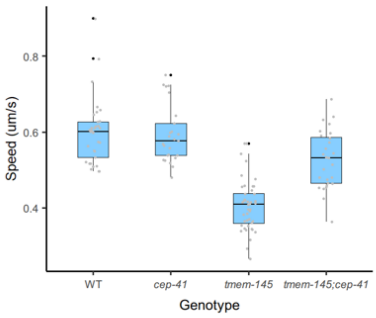

Test of Normality (Shapiro-Wilk)

	W	p
Speed	0.955	< .001

Note. A low p-value suggests a violation of the assumption of normality

One-Way ANOVA (Fisher's)

	F	df1	df2	p
Speed	52.2	3	125	< .001

Test for Equality of Variances (Levene's)

	F	df1	df2	p
Speed	0.446	3	125	0.721

Group Descriptives

	Genotype	N	Mean	SD	SE
Speed	WT	33	0.599	0.0864	0.0150
	cep-41	25	0.593	0.0766	0.0153
	tmem-145	44	0.406	0.0670	0.0101
	tmem-145; cep-41	27	0.526	0.0768	0.0148

C)

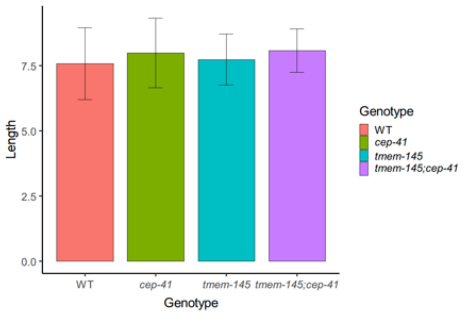

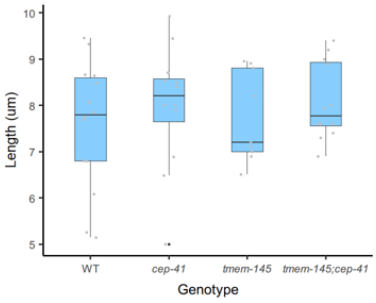

Test of Normality (Shapiro-Wilk)

	W	p
Length	0.972	0.323

Note. A low p-value suggests a violation of the assumption of normality

One-Way ANOVA (Welch's)

	F	df1	df2	p
Length	0.508	3	22.8	0.681

Test for Equality of Variances (Levene's)

	F	df1	df2	p
Length	0.834	3	43	0.483

Group Descriptives

	Genotype 2	N	Mean	SD	SE
Length	Wild Type	14	7.57	1.382	0.369
	cep-41	12	7.98	1.332	0.385
	tmem-145	9	7.73	0.977	0.326
	tmem-145;cep-41	12	8.07	0.837	0.241

Figure 3.3.7 OSM-6::GFP localization is not affected in *tmem-145* mutant worms but IFT is slower in *tmem-145(tur002)* mutants.

(A) Representative images of phasmid and amphid cilia of wild type, *tmem-145(tur002)* and *cep-41* single, and *tmem-145(tur002); cep-41* double mutants are shown. Scale bars are 2 μm. (B) Barplot and boxplot showing length of the cilia in these four genotypes. The data was assessed on normality and equality of variance. Since the data is not normally distributed nor has equal variance, Welch's one-way ANOVA test was applied. (C) Barplot and boxplot of IFT speeds for these four genotypes. Test of normality and varience equality was performed. Fisher's one-way ANOVA was applied because of the normal distribution. (D) Kymographic analysis of IFT speeds. On the left is representative image of cilia used for kymograph. On the right is representative kymograph image with lines used for calculations.

3.4 Localizations of Membrane Proteins Are Not Disrupted in *tmem-145(tur002)* Mutants

Although TMEM-145 is not required for ciliogenesis, we thought that *tmem-145(tur002)* mutation may lead to disrupted localization of transmembrane proteins. To test this hypothesis, we have generated *him-5;tmem-145(tur002);*[PKD-2::GFP] transgenic worms to both examine CEM cilia structure and localization of PKD-2::GFP chimeric protein in *tmem-145(tur002)* mutants. PKD-2 encodes the polycystic kidney disease 2 (PKD2) membrane protein and is exclusively expressed in the male ciliated sensory neurons. GFP tagged PKD-2 is well known to localize to the cilia with most of the signal is seen in the cell body. Analysis with fluorescent microscopy has revealed that PKD-2::GFP localization in CEM cilia of tales in male *him-5;tmem-145(tur002)* mutant worms was the same with wild type worms (Figure 3.4.1A). However, interestingly, in head of *him-5;tmem-145(tur002)* mutants, PKD-2::GFP was more abundant than in head of wild type worms (Figure 3.4.1B). This was measured by comparing ratios of fluorescent intensity between cilia and cell body. This means that in *him-5;tmem-145(tur002)* mutants, more PKD-2::GFP was localized to head cilia compared to wild type worms.

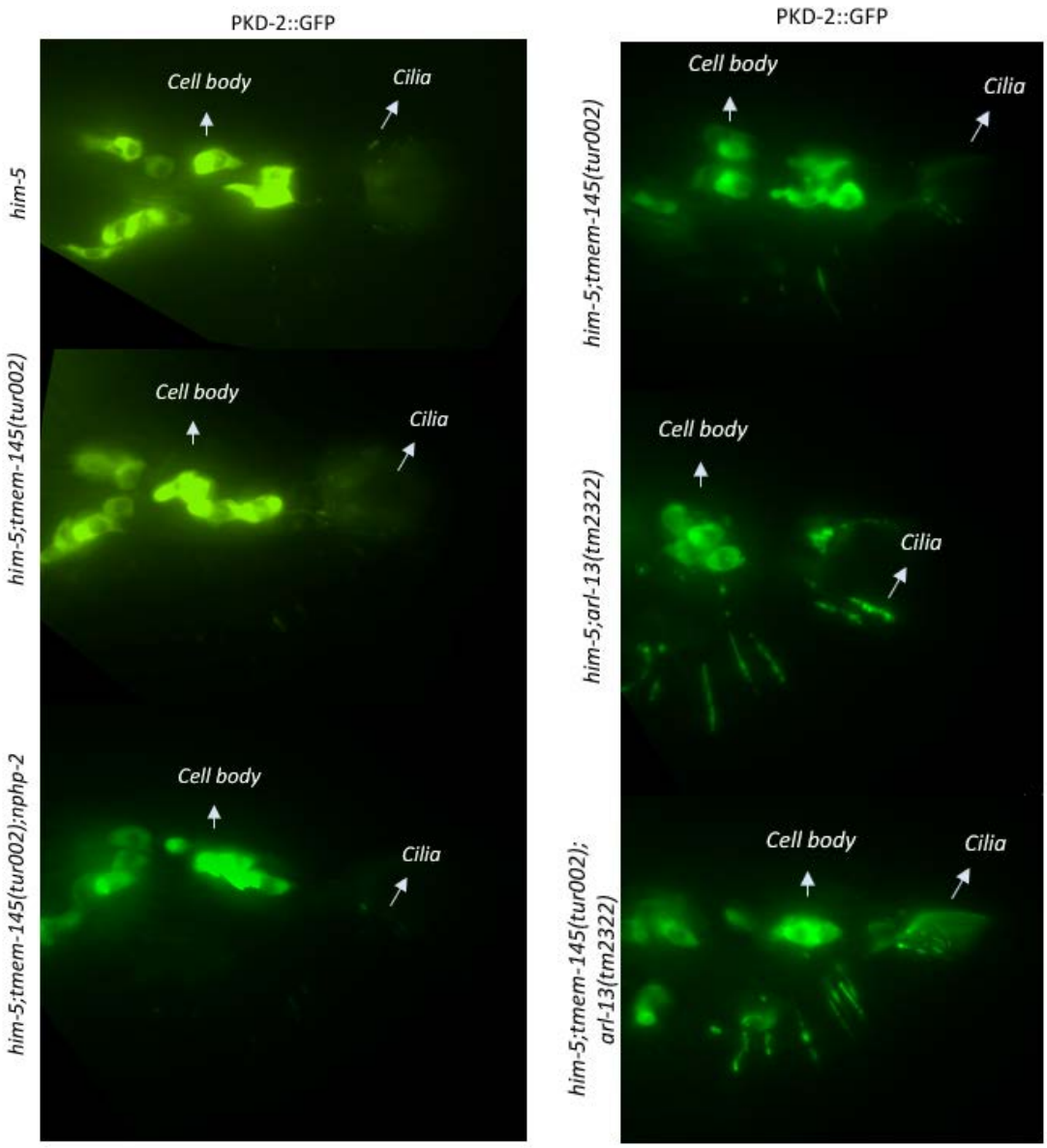

Figure 3.4.1 *C. elegans* single *tmem-145(tur002)* mutants exhibit normal PKD-2 localization in CEM cilia in male worms.

Representative fluorescent images from wild type, *him-5;tmem-145(tur002)*, *him-5;tmem-145(tur002);nphp-2, him-5;arl-13(tm2322)*, *him-5;tmem-145(tur002);arl-13(tm2322)* worms are shown. Arrows show PKD-2 localization in CEM cell body and CEM cilia for comparison of fluorescent intensity of cilia and cell body.

A)

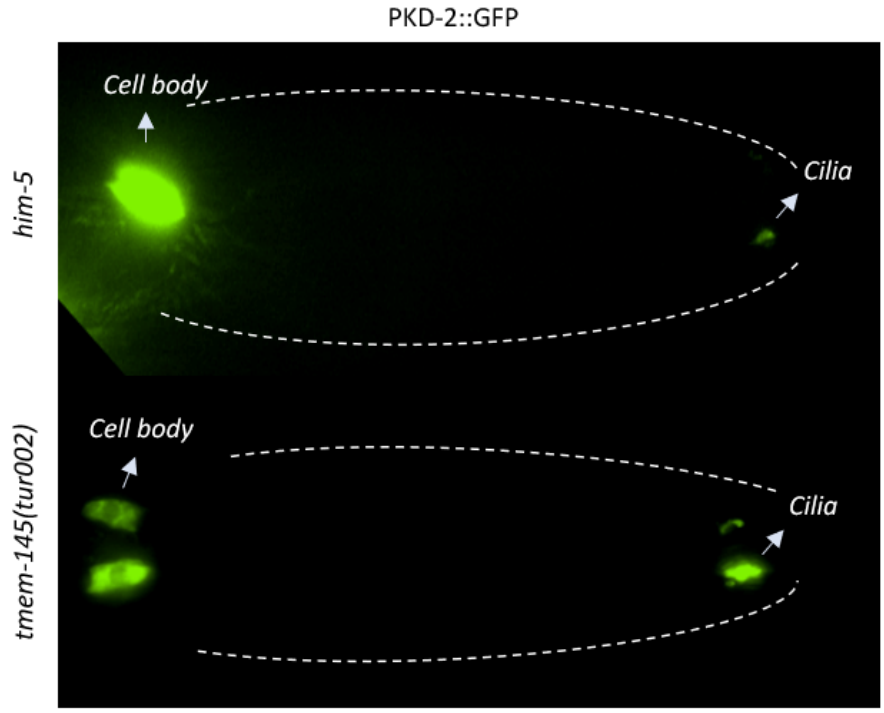

B)

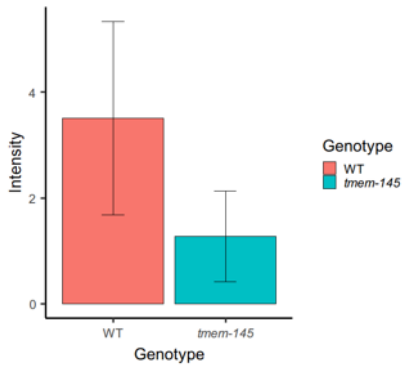

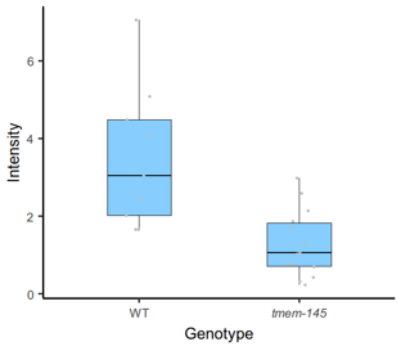

Tests of Normality

		statistic	p
Intensity	Shapiro-Wilk	0.946	0.241
	Kolmogorov-Smirnov	0.128	0.800
	Anderson-Darling	0.349	0.443

Note. Additional results provided by *moretests*

Independent Samples T-Test

		statistic	df	p	Mean difference	SE difference
Intensity	Welch's t	3.42	10.3	0.006	2.23	0.651

Test of Equality of Variances (Levene's)

	F	df	df2	p
Intensity	7.60	1	21	0.012

Note. A low p-value suggests a violation of the assumption of equal variances

Group Descriptives

	Group	N	Mean	Median	SD	SE
Intensity	WT	9	3.50	3.04	1.83	0.610
	tmem-145	14	1.28	1.05	0.857	0.229

Figure 3.4.2: *C. elegans* single *tmem-145(tur002)* mutants show excess PKD-2 accumulation in CEM cilia in male worms.

(A) Representative images from wild type and *tmem-145* mutant worms are shown. Arrows show PKD-2 localization in CEM cell body and CEM cilia for comparison of fluorescent intensity of cilia and cell body. (B) Barplot and boxplot showing the intensity ratio of cilia and cell body in WT and *tmem-*

145(tur002) mutant. Normality and equality of variance tests was applied. Welch's T-test was used to determine the significance of difference between cilia/cell body intensity ratios in WT and *tmem-145(tur002)* worms.

3.5 Double Mutant Analysis

Based on exclusive cilia localization, we predicted that TMEM-145 would play a role in ciliogenesis either directly, or through regulating other components of cilia biogenesis. However, close inspection of generated *tur002* mutant led us to conclude two hypothesis. First, lack of a clear ciliary phenotype may suggest that there might be functional redundancy in the pathways in which *tmem-145* functions in cilia biogenesis, meaning that other genes may compensate the lack of *tmem-145*. Second, *tmem-145* (*tur002)* mutant may not be a null allele of *tmem-145*.

In order to test the first hypothesis, we have generated double mutants consisting of *tmem-145(tur002)* and genes encoding proteins that localize to the middle segment of cilia or transition zone. These genes include *nphp-4* (Human NPHP4), *arl-13* (Human ARL13B), mks-5 (Human RPGRIP1L) and *bbs-5* (Human BBS5). We first obtained the mutants of these genes and then employed the Dye filling assay and fluorescence markers that label cilia to test genetic interactions between *tmem-145* and these genes. The dye filling assays revealed that none of double mutants (*tmem-145(tur002);nphp-4(tm925) tmem-145(tur002);bbs-5(tm3100)* and *tmem-145(tur002);nphp-4(tm925)* and *bbs-5(tm3100)* single possess additive ciliary phenotype (Figure 3.3.2). Then we have examined the structure of PHA/ PHB cilia (marker used *srb-6p::gfp*) in *tmem-145(tur002);arl-13(gk513), tmem-145(tur002);nphp-4(tm925) and tmem-145(tur002);mks-5(tm3100)* double mutants. No additive phenotype was observed in *tmem-145(tur002);nphp-4(tm925) and tmem-145(tur002);mks-5(tm3100)* double mutants and the phenotype in *tmem-145(tur002);arl-13(gk513)* double mutant was the same as *arl-13(gk513)* single mutant, which has shown kinky phenotype in PHA/B cilia (Figure 3.3.3).

In order to assess a possible functional redundancy between *tmem-145(tur002)* and *grk-2* genes, we have generated *tmem-145(tur002),grk-2* in transgenic worms having

str-1p::gfp to examine the structure of AWB cilia. GRK-2 is a G protein coupled receptor kinase protein and it has been shown that *grk-2* mutant *C. elegans* is defective in their AWB cilia structure, with fan-like shape at tip of the cilia [40]. Worms with *tmem-145(tur002);grk-2* double mutant exhibited *grk-2* mutant-like AWB cilia structure, suggesting that there is no functional redundancy between *tmem-145(tur002)* and *grk-2* (Figure 3.3.4).

Next, we have examined OSM-6::GFP localization in *tmem-145(tur002);cep-41(tur001)* double mutant to see if *tmem-145(tur002)* and *cep-41* are functionally redundant. Interestingly, double mutants have rescued the slow OSM-6::GFP movement in middle segment of *tmem-145(tur002)* single mutant (Figure 3.3.6C). Structurally however, there is no difference between double mutant and wild type phasmid and amphid cilia (Figure 3.3.6A).

3.6 Generation of Null Mutant Allele of *tmem-145*

Given that *tmem-145(tur002)* mutant may not be null, we used CRISPR/Cas9 to generate a new null for *tmem-145.* We designed and cloned three sgRNAs targeting exon 1, 8 and 11 in *tmem-145.* We performed microinjection of three sgRNAs together with Cas9 plasmids and a selection marker. We then used the PCR strategy coupled with Sanger sequencing to screen a new *tmem-145* mutant. We found a mutant with a 2110 bp deletion and named mutant allele *tur009* (Figure 3.6.1C). Sanger sequencing revealed that exon 1-8, 10 and most part of exon 11 was removed in *tur009* mutant (Figure 3.6.1A-B). In addition, most part of Rhodopsin-like GPCR transmembrane domain (GpcrRhopsn4) was also removed (Figure 3.6.1D). The remaining exons were not in-frame; suggesting a strong possibility of being a null allele. Due to the limited time frame, we have not been able to examine *tmem-145(tur009)* allele thoroughly. We have generated *tmem-145(tur009);[str-1p::mCherry]* strain to look at AWB cilia and observed that the single mutants were structurally the same with wild type worms (Figure 3.6.2).

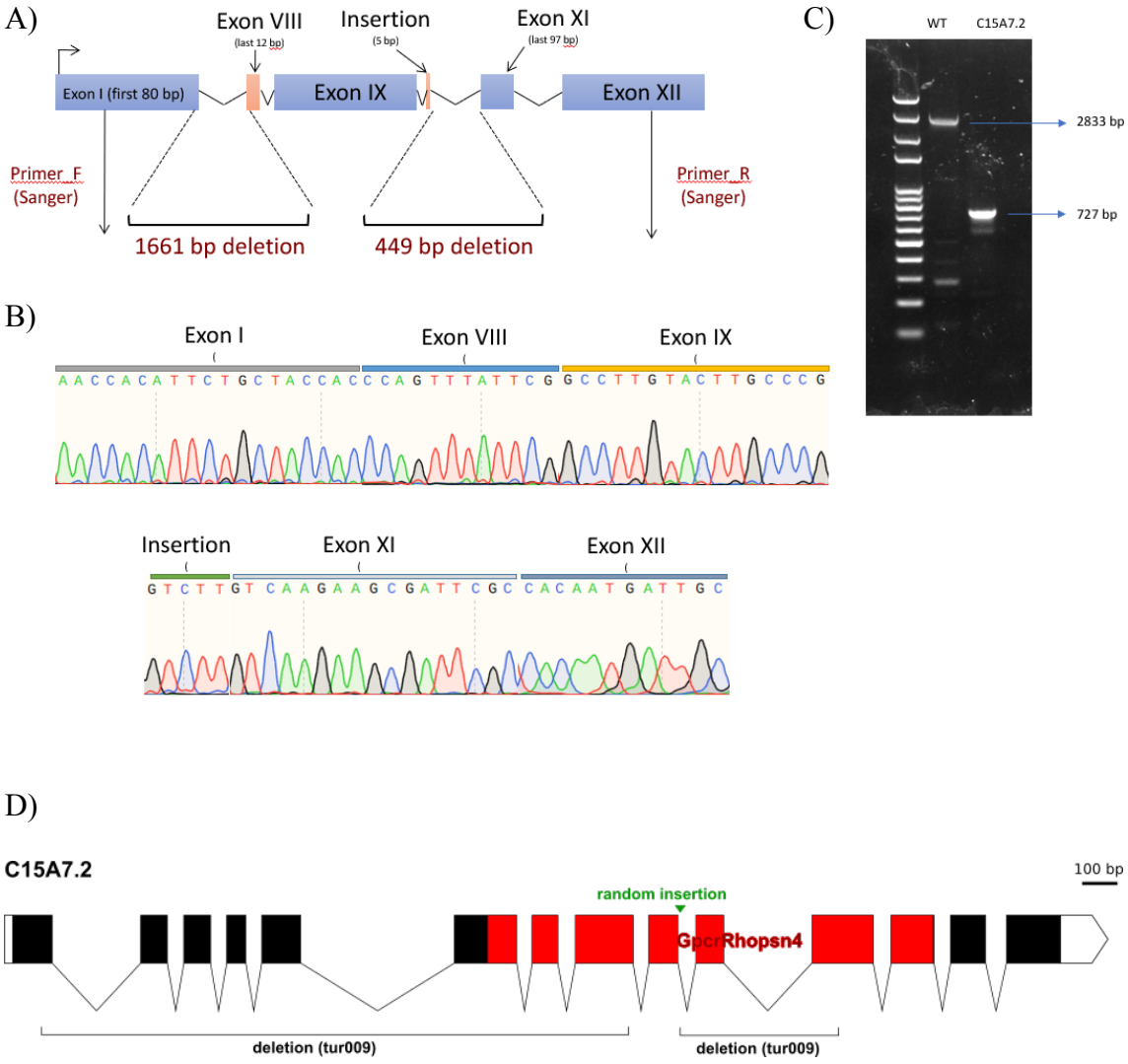

Figure 3.6.1 Schematic structure of *tmem-145(tur009)* allele

(A) Representation of *tmem-145(tur009)* allele structure showing exons, introns, deletions, insertion and primers used for sanger sequencing. (B) Representation of sanger sequencing result for *tmem-145(tur009)* allele. (C) Electrophoresis image showing wild type and *tmem-145(tur009)* allele length. (D) Scaled schematic representation of *tmem-145(tur009)* allele showing all exons, introns, insertion and deletions.

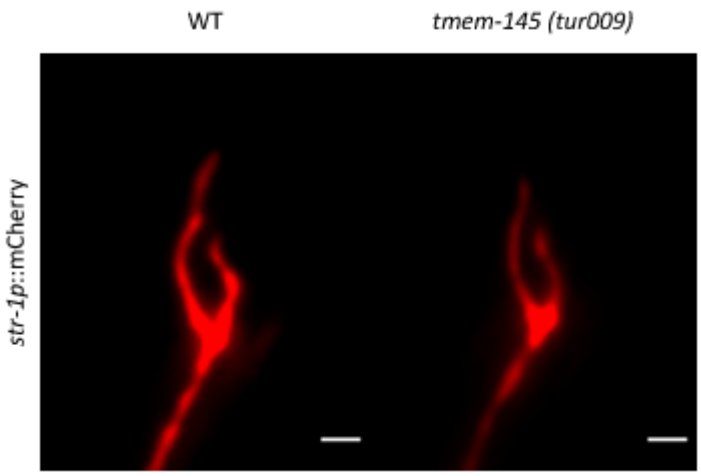

Figure 3.6.2 AWB cilia in *tmem-145(tur009)* allele are structurally same with wild type cilia.

Shown are representative images of AWB cilia in wild type and *tmem-145(tur009)* mutants. AWB cilia have a fork-like shape. The shape appears to be unaffected in *tmem-145(tur009)* mutants. *str-1p*::mCherry was used to monitor AWB cilia. Scale bars are 2 µm.

Chapter 4

Discussion

To date, more than 600 proteins have been identified in ciliary axoneme [41] and among the genes that are coding these proteins, more than 200 have been associated with ciliopathies [3]. Therefore, there is a constant need for deciphering novel ciliary and ciliopathy associated genes. The Kaplan lab has been working on predicting new ciliary genes through single-cell RNA-seq. They have identified a couple of candidate genes, one of which was *C. elegans C15A7.2* gene encoding a GPCR protein, which we named as TMEM-145. Single cell RNA-seq analysis revealed that *tmem-145* is expressed only ciliated neurons in *C. elegans*. Therefore, I have started to characterize this gene.

Cilia possess numerous sub-compartments including basal body (BD), transition zone (TZ) and middle segment (MS). Each compartment contains a specific set of genes, each having specific functions with other genes forming different modules. Determining subcellular localization of a protein is essential in functional characterization of novel protein due to the effect of environment in which the protein operates, on the function by managing access to interacting proteins [42]. As such, we have investigated the subcellular localization of *C15A7.2* coding protein, which we named as TMEM-145 in *C. elegans* and found that it exclusively localizes to middle segment of both head and tail sensory neurons in *C. elegans*. This makes TMEM-145 one of the middle segment protein family members, which also includes CEP41(unpublished data), ARL-13 and NPHP-2 (inversin) [43], [44].

It is known that some of other known ciliary middle segment protein coding genes such as *arl-13* and *nphp-2* interact with each other to regulate ciliogenesis [45], so *tmem-145* may also interact one or more of these proteins. In addition, the proteins regulating glutamylation of microtubules are known to regulate localization and abundance of

membrane proteins, like PKD-2 [46], so it might be possible for TMEM-145 to be involved in glutamylation process and regulate ciliary abundance and localization of these proteins. Moreover, having found that TMEM-145 has a transmembrane domain; it is important to investigate the effect of TMEM-145 on other membrane proteins.

It has been previously shown that CEP41, a Joubert Syndrome associated protein, is necessary for tubulin glutamylation [47], and *C. elegans* ortholog of human *CEP41* gene *F42G8.19* coding protein has been found to be localized to middle segment of cilia, similar to TMEM-145 (unpublished data). We thought that in a similar manner with the interaction between *ttll-11* and *ccpp-1* [46]; *cep-41* and *tmem-145* might regulate tubulin glutamylation. Since defects in glutamylation of ciliary tubulins lead to change in kinesin-II velocity [46], we have examined the OSM-6 velocity in both single and double mutants of *tmem-145(tur002)* and *cep-41(tur001)*. The decrease in OSM-6 velocity in *tmem-145(tur002)* single mutant may indicate a crucial role of TMEM-145 protein in tubulin glutamylation. In addition, we have found that *tmem-145(tur002);cep-41(tur001)* double mutants rescue the phenotype which had been observed in *tmem-145(tur002)* single mutants, suggesting that *tmem-145(tur002)* might be antagonized by *cep-41(tur001)*. Since it may also affect OSM-6 speed in a different pathway, further investigation is required to safely claim that *tmem-145(tur002)* affects glutamylation.

Many GPCRs are localized to cilia and many research on ciliopathies suggest that GPCR signaling through cilia plays key role in many cellular and developmental pathways [28]. For example, Hedgehog (Hh) signaling which is essential in human development, dependent on cilia [48]. It has been shown that the proteins essential for Hh signaling are localized to cilia and their abundance change during signaling [48]. One such protein is a seven transmembrane protein SMO, which is expressed and localized to cilia during Hh signaling and in the absence of this protein, Hh signaling pathway activity is disrupted [49]. Due to its Rhodopsin-like GPCR transmembrane domain (GpcrRhopsn4), we suggest that TMEM-145 is a G protein coupled receptor. Therefore, it is necessary to investigate if *tmem-145* function in a ciliary GPCR pathway such as olfactory receptor signaling and hedgehog signaling pathways.

To fully characterize *tmem-145*, we have examined its role in cilia biogenesis by looking at the effect of *tmem-145(tur002)* mutation on the structure of different cilia types. Having cilia specific expression and middle segment localization, *tmem-145* is expected

to have significant impact on cilia biogenesis, therefore, the disruption of it would cause defects in cilia structure. We have analyzed the structures of PHA/B, AWB and OLQ cilia of wild type and *tmem-145(tur002)* mutant worms and cilia structures of *tmem-145(tur002)* mutants were the same with wild type. Dye filling assay also did not result in a phenotype, indicating that *tmem-145(tur002)* mutant worms have functional and undisrupted cilia.

Ciliary abundance of PKD-2 affects the sensory functions, and thus regulated by a number of genes such as *klp-6* and *arl-13* [43], [50], [51]. In addition, in *C. elegans*, the localization and abundance of PKD-2 affects male mating behavior [51]. Therefore, we have analyzed the localization of PKD-2 in *tmem-145(tur002)* mutant worms and although PKD-2 have excessive localization on head cilia, the cilia in tale of male *tmem-145(tur002)* mutant worms exhibit the same PKD-2 localization with wild type. Being absent of any result regarding head cilia specific abundance of PKD-2 in literature, we have concluded that this finding is required to be further explored.

There might be a couple of reasons why although TMEM-145 is exclusively located in cilia and a transmembrane protein with rhodopsin domain, it does not exhibit any defects in cilia structure and function. First, there might be genes that *tmem-145* is functionally redundant with. Williams et al. have found that MKS and NPHP proteins form an interaction network that regulates ciliogenesis and they are separated into modules, in which double mutations of the genes from same modules do not disrupt ciliogenesis and only in the absence of genes from different modules results in disruption of ciliogenesis and exhibits phenotype [52]. This indicates how functional redundancy leads to not observing any phenotype when one or more ciliary genes are disrupted. We have generated and examined *tmem-145;arl-13, tmem-145;nphp-2, tmem-145;cep-41 and tmem-145;bbs-5* double mutants to see if functional redundancy is the reason why *tmem-145(tur002)* allele does not exhibit any particular, strong phenotype. Apart from *tmem-145;cep-41* double mutant, other strains exhibit wild type phenotype. Therefore, there might be other genes that *tmem-145* is redundant with, and BLAST analysis of TMEM-145 has revealed that another GPCR transmembrane protein T04F8.4, an ortholog of human GPR180 protein has 31.8% similarity to TMEM-145 (unpublished) and has the same rhodopsin-like domain, indicating that they might be functionally redundant. Therefore, more double mutant combinations including one with T04F8.4 are required to fully characterize ciliary function of TMEM145 protein.

The second reason might be that *tmem-145(tur002)* mutant may not be null, as there is no frameshift in remaining polypeptide after removing first four exons of the gene. Considering that no part of the rhodopsin-like GPCR transmembrane domain of TMEM-145 protein is removed in *tmem-145(tur002)* mutants, it is highly probable that *tmem-145(tur002)* mutant allele is not null, thus might still be functioning. In order to confirm this hypothesis, TMEM-145(TUR002)::GFP transgenic worms should be generated to see if this mutant protein still localizes to cilia like TMEM-145::GFP does.

Due to the possibility for *tmem-145(tur002)* of not being null, we have generated another *tmem-145* allele, *tur009*. We have removed 2110 bp corresponding to exon 1-8, 10 and a part of exon 11, which remove most of the Rhodopsin-like GPCR transmembrane domain and cause frameshift. However, due to the limited time, we have only generated *tmem-145(tur009);[str-1p::tdTomato]* transgenic strain to examine the structure of AWB cilia. This allele shows no phenotype and has the same AWB cilia structure with wild type therefore further investigation is required.

Chapter 5

Conclusions and Future Prospects

5.1 Conclusions

In this study, we wished to characterize a potentially ciliary gene *tmem-145* in *C. elegans*. We have found that *C15A7.2* gene, which is homolog to human *TMEM145* and which we named as *tmem-145*, is expressed only in ciliated sensory neurons in *C. elegans* and localizes only to middle segment of amphid and phasmid cilia. We have also found that OSM-6::GFP speed in *tmem-145(tur002)* mutants is significantly decreased and double mutant with *cep-41(tur001)* allele has OSM-6::GFP speed similar to wild type. This may suggest that TMEM-145 may have a role in polyglutamylation of microtubules. We haven't found any structural defect in any of the single and double mutants. Later, we have suspected that *tmem-145(tur002)* mutant may not be null, therefore we have generated a new allele *tmem-145(tur009)*. This mutant has successfully uptaken dye in dyf assay and have not showed any structural defects in AWB cilia, suggesting that both amphid, phasmid and AWB cilia structures are not severely affected by *tmem-145(tur009)* mutant.

5.2 Contribution to Global Sustainability

Ciliopathies consist of a range of diseases affecting millions of people worldwide. In order to decipher the underlying mechanism of ciliopathies, genetic mechanism of structure and function of the cilia are required to be fully explored. Most of the ciliopathies are caused by the mutations in the genes which are necessary for proper function of cilia and the ones which are required in cilia integrity. Although currently there is no cure for most of the ciliopathies, knowing the disease-causing mutations in ciliary genes could prevent birth of individuals with ciliopathies by testing parents whether if they carry any ciliopathy related mutations. Therefore, it is necessary to find novel genes affecting cilia integrity and function to fully understand the causes and prevent ciliopathies. We have found that *tmem-145* is a ciliary gene encoding a protein which is exclusively expressed in ciliary cells and localized to cilia in *C. elegans*. Since *tmem-145* is conserved in human as well, it is possible that human *TMEM145* is also a ciliary gene. Although further research is required to fully understand the function of TMEM145, our research would be a valuable starting point to uncover a novel ciliary protein and a potential target for preventing ciliopathies.

5.3 Future Prospects

C. elegans TMEM-145 protein has been found to be exclusively localized in middle segment of the cilia. However, it is not known if human TMEM145 protein also localized to cilia. Therefore, it is necessary to confirm subcellular localization of human TMEM145.

Although our analysis showed that *tmem-145(tur002)* mutation affects IFT speed, by which pathway it affects IFT is not yet known. Therefore, more double mutant analysis with genes affecting IFT, like *ttll-11* and *ccpp-1* are required.

We have suggested that TMEM-145 may be a G-protein coupled receptor and therefore its function in GPCR pathways can be investigated by both exploring protein and genetic interactions of TMEM145 with ciliary GPCR pathway proteins such as GPR161 and GPR175.

Our work revealed that PKD-2 localization is not affected in *tmem-145(tur002)* single and various double mutants. However, due to the possibility of a functional

redundancy with genes affecting PKD-2 localization that we have not analyzed, such as *klp-6*; double mutants with these genes should be analyzed.

Most importantly, since the *tmem-145(tur002)* allele may not be null; TMEM-145(TUR002)::GFP transgenic worms should be generated to see if *tur002* allele is functional. If *tur002* allele is not null, TMEM-145(TUR009)::GFP transgenic strain should be generated to confirm the newly generated *tmem-145(tur009)* mutant strain is null. If it is null, then same experiments should be performed to characterize *tmem-145* gene.

BIBLIOGRAPHY

[1] J. M. Pan, “Cilia and ciliopathies: From Chlamydomonas and beyond,” *Sci. China, Ser. C Life Sci.*, vol. 51, no. 6, pp. 479–486, 2008.

[2] W. F. Marshall, *Chapter 1 Basal Bodies. Platforms for Building Cilia*, 1st ed., vol. 85, no. 08. Elsevier Inc., 2008.

[3] J. F. Reiter and M. R. Leroux, “Genes and molecular pathways underpinning ciliopathies,” *Nat. Rev. Mol. Cell Biol.*, vol. 18, no. 9, pp. 533–547, 2017.

[4] J. M. Brown and G. B. Witman, “Cilia and diseases,” *BioScience*. 2014.

[5] S. C. Goetz and K. V. Anderson, “The primary cilium: A signalling centre during vertebrate development,” *Nature Reviews Genetics*. 2010.

[6] V. Singla and J. F. Reiter, “The primary cilium as the cell’s antenna: Signaling at a sensory organelle,” *Science (80-.).*, vol. 313, no. 5787, pp. 629–633, 2006.

[7] M. A. Zariwala, M. R. Knowles, and H. Omran, “Genetic Defects in Ciliary Structure and Function,” *Annu. Rev. Physiol.*, vol. 69, no. 1, pp. 423–450, 2007.

[8] B. Chih *et al.*, “A ciliopathy complex at the transition zone protects the cilia as a privileged membrane domain,” *Nat. Cell Biol.*, vol. 14, no. 1, pp. 61–72, 2012.

[9] Y. C. Hsiao, K. Tuz, and R. J. Ferland, “Trafficking in and to the primary cilium,” *Cilia*, vol. 1. 25-Apr-2012.

[10] B. Craige *et al.*, “CEP290 tethers flagellar transition zone microtubules to the membrane and regulates flagellar protein content,” *J. Cell Biol.*, vol. 190, no. 5, pp. 927–940, Sep. 2010.

[11] G. Garcia, D. R. Raleigh, and J. F. Reiter, “How the Ciliary Membrane Is Organized Inside-Out to Communicate Outside-In,” *Curr. Biol.*, vol. 28, no. 8, pp. R421–R434, 2018.

[12] J. Lee and Y. D. Chung, “Ciliary subcompartments: How are they established and what are their functions?,” *BMB Reports*, vol. 48, no. 7. The Biochemical Society of the Republic of Korea, pp. 380–387, 2015.

[13] H. Soares, B. Carmona, S. Nolasco, L. Viseu Melo, and J. Gonçalves, “Cilia Distal Domain: Diversity in Evolutionarily Conserved Structures,” *Cells*, vol. 8, no. 2, p. 160, Feb. 2019.

[14] P. N. Inglis, G. Ou, M. R. Leroux, and J. M. Scholey, “The sensory cilia of

Caenorhabditis elegans.," *WormBook*, pp. 1–22, 2007.

[15] A. Metaxakis, D. Petratou, and N. Tavernarakis, "Multimodal sensory processing in Caenorhabditis elegans," *Open Biology*, vol. 8, no. 6. Royal Society Publishing, 01-Jun-2018.

[16] A. K. Corsi, B. Wightman, and M. Chalfie, "A Transparent window into biology: A primer on Caenorhabditis elegans," *WormBook*, pp. 1–31, 2015.

[17] M. Klass and D. Hirsh, "Non-ageing developmental variant of Caenorhabditis elegans," *Nature*, vol. 260, no. 5551, pp. 523–525, 1976.

[18] K. G. Kozminski, K. A. Johnson, P. Forscher, and J. L. Rosenbaum, "A motility in the eukaryotic flagellum unrelated to flagellar beating," *Proc. Natl. Acad. Sci. U. S. A.*, vol. 90, no. 12, pp. 5519–5523, 1993.

[19] J. L. Rosenbaum and G. B. Witman, "Intraflagellar transport," *Nature Reviews Molecular Cell Biology*. 2002.

[20] Z. Walther, M. Vashishtha, and J. L. Hall, "The Chlamydomonas FLA10 gene encodes a novel kinesin-homologous protein," *J. Cell Biol.*, vol. 126, no. 1, pp. 175–188, Jul. 1994.

[21] F. Hildebrandt, T. Benzing, and N. Katsanis, "Ciliopathies," *New England Journal of Medicine*, vol. 364, no. 16. Massachussetts Medical Society, pp. 1533–1543, 21-Apr-2011.

[22] Y. Okada, S. Nonaka, Y. Tanaka, Y. Saijoh, H. Hamada, and N. Hirokawa, "Abnormal nodal flow precedes situs inversus in iv and inv mice," *Mol. Cell*, vol. 4, no. 4, pp. 459–468, Oct. 1999.

[23] M. M. Barr and P. W. Sternberg, "A polycystic kidney-disease gene homologue required for male mating behaviour in C. elegans," *Nature*, vol. 401, no. 6751, pp. 386–389, Sep. 1999.

[24] G. Wheway, D. A. Parry, and C. A. Johnson, "The role of primary cilia in the development and disease of the retina," *Organogenesis*, vol. 10, no. 1. Landes Bioscience, pp. 69–85, 2014.

[25] D. P. McEwen, P. M. Jenkins, and J. R. Martens, *Chapter 12 Olfactory Cilia: Our Direct Neuronal Connection to the External World*, 1st ed., vol. 85, no. 08. Elesvier Inc., 2008.

[26] M. M. Kunte *et al.*, "ER stress is involved in T17M rhodopsin-induced retinal degeneration," *Investig. Ophthalmol. Vis. Sci.*, vol. 53, no. 7, pp. 3792–3800, Jun. 2012.

[27] D. M. Rosenbaum, S. G. F. Rasmussen, and B. K. Kobilka, "The structure and function of G-protein-coupled receptors," *Nature*, vol. 459, no. 7245, pp. 356–363, 2009.

[28] K. Mykytyn and C. Askwith, "G-Protein-Coupled receptor signaling in cilia," *Cold Spring Harb. Perspect. Biol.*, vol. 9, no. 9, pp. 1–15, 2017.

[29] K. I. Hilgendorf, C. T. Johnson, and P. K. Jackson, "The primary cilium as a cellular receiver: Organizing ciliary GPCR signaling," *Curr. Opin. Cell Biol.*, vol. 39, pp. 84–92, 2016.

[30] O. Smithies, R. G. Gregg, S. S. Boggs, M. A. Koralewski, and R. S. Kucherlapati, “Insertion of DNA sequences into the human chromosomal β-globin locus by homologous recombination,” *Nature*, vol. 317, no. 6034, pp. 230–234, 1985.

[31] M. Adli, “The CRISPR tool kit for genome editing and beyond,” *Nature Communications*, vol. 9, no. 1. Nature Publishing Group, pp. 1–13, 01-Dec-2018.

[32] J. D. Sander and J. K. Joung, “CRISPR-Cas systems for editing, regulating and targeting genomes,” *Nature Biotechnology*, vol. 32, no. 4. Nature Publishing Group, pp. 347–350, 02-Mar-2014.

[33] L. Cong *et al.*, “Multiplex genome engineering using CRISPR/Cas systems,” *Science (80-.).*, vol. 339, no. 6121, pp. 819–823, Feb. 2013.

[34] Y. Ishino, H. Shinagawa, K. Makino, M. Amemura, and A. Nakata, “Nucleotide Sequence of the iap Gene, Responsible for Alkaline Phosphatase Isozyme Conversion in Escherichia coli, and Identification of the Gene Product,” 1987.

[35] R. Barrangou *et al.*, “CRISPR provides acquired resistance against viruses in prokaryotes,” *Science (80-.).*, vol. 315, no. 5819, pp. 1709–1712, Mar. 2007.

[36] E. Deltcheva *et al.*, “CRISPR RNA maturation by trans-encoded small RNA and host factor RNase III,” *Nature*, vol. 471, no. 7340, pp. 602–607, Mar. 2011.

[37] S. Waaijers *et al.*, “CRISPR/Cas9-targeted mutagenesis in Caenorhabditis elegans,” *Genetics*, vol. 195, no. 3. Genetics Society of America, pp. 1187–1191, 2013.

[38] P. LA, H. EM, T. JN, and C. JG, “Mutant sensory cilia in the nematode C. elegans.,” *Dev. Biol.*, vol. 117, pp. 456–487, 1986.

[39] Y. K. Bae and M. M. Barr, “Sensory roles of neuronal cilia: Cilia development, morphogenesis, and function in C. elegans,” *Front. Biosci.*, vol. 13, no. 15, pp. 5959–5974, May 2008.

[40] S. Mukhopadhyay, Y. Lu, S. Shaham, and P. Sengupta, “Sensory Signaling-Dependent Remodeling of Olfactory Cilia Architecture in C. elegans,” *Dev. Cell*, vol. 14, no. 5, pp. 762–774, May 2008.

[41] G. J. Pazour, N. Agrin, J. Leszyk, and G. B. Witman, “Proteomic analysis of a eukaryotic cilium,” *J. Cell Biol.*, vol. 170, no. 1, pp. 103–113, Jul. 2005.

[42] M. S. Scott, S. J. Calafell, D. Y. Thomas, and M. T. Hallett, “Refining protein subcellular localization,” *PLoS Comput. Biol.*, vol. 1, no. 6, pp. 0518–0528, 2005.

[43] S. Cevik *et al.*, “Joubert syndrome Arl13b functions at ciliary membranes and stabilizes protein transport in Caenorhabditis elegans.,” *J. Cell Biol.*, vol. 188, no. 6, pp. 953–69, Mar. 2010.

[44] S. R. F. Warburton-Pitt, A. R. Jauregui, C. Li, J. Wang, M. R. Leroux, and M. M. Barr, “Ciliogenesis in Caenorhabditis elegans requires genetic interactions between ciliary middle segment localized nphp-2 (inversin) and transition zoneassociated proteins,” *J. Cell Sci.*, vol. 125, no. 11, pp. 2592–2603, Jun. 2012.

[45] S. R. F. Warburton-Pitt, M. Silva, K. C. Q. Nguyen, D. H. Hall, and M. M. Barr,

"The nphp-2 and arl-13 Genetic Modules Interact to Regulate Ciliogenesis and Ciliary Microtubule Patterning in C. elegans," *PLoS Genet.*, vol. 10, no. 12, p. e1004866, Dec. 2014.

[46] R. O'Hagan *et al.*, "Glutamylation Regulates Transport, Specializes Function, and Sculpts the Structure of Cilia," *Curr. Biol.*, vol. 27, no. 22, pp. 3430-3441.e6, Nov. 2017.

[47] J. E. Lee *et al.*, "CEP41 is mutated in Joubert syndrome and is required for tubulin glutamylation at the cilium," *Nat. Genet.*, vol. 44, no. 2, pp. 193–199, Feb. 2012.

[48] F. Bangs and K. V. Anderson, "Primary cilia and Mammalian Hedgehog signaling," *Cold Spring Harb. Perspect. Biol.*, vol. 9, no. 5, May 2017.

[49] K. C. Corbit, P. Aanstad, V. Singla, A. R. Norman, D. Y. R. Stainier, and J. F. Reiter, "Vertebrate Smoothened functions at the primary cilium," *Nature*, vol. 437, no. 7061, pp. 1018–1021, Oct. 2005.

[50] E. M. Peden and M. M. Barr, "The KLP-6 kinesin is required for male mating behaviors and polycystin localization in Caenorhabditis elegans," *Curr. Biol.*, vol. 15, no. 5, pp. 394–404, Mar. 2005.

[51] Y. K. Bae, H. Qin, K. M. Knobel, J. Hu, J. L. Rosenbaum, and M. M. Barr, "General and cell-type specific mechanisms target TRPP2/PKD-2 to cilia," *Development*, vol. 133, no. 19, pp. 3859–3870, Oct. 2006.

[52] C. L. Williams *et al.*, "MKS and NPHP modules cooperate to establish basal body/transition zone membrane associations and ciliary gate function during ciliogenesis," *J. Cell Biol.*, vol. 192, no. 6, pp. 1023–1041, Mar. 2011.

[53] Schindelin, J., Arganda-Carreras, I., Frise, E.*et al.*Fiji: an open-source platform for biological-image analysis.*Nat Methods***9,**676–682 (2012).

[54] Rueden, C.T., Schindelin, J., Hiner, M.C.*et al.*ImageJ2: ImageJ for the next generation of scientific image data.*BMC Bioinformatics***18,**529 (2017)

[55] Waterhouse, A. M., Procter, J. B., Martin, D. M., Clamp, M., & Barton, G. J. Jalview Version 2--a multiple sequence alignment editor and analysis workbench.*Bioinformatics (Oxford, England)*,*25*(9), 1189–1191 (2009)

[56] The jamovi project (2020). *jamovi*. (Version 1.2) [Computer Software]. Retrieved from https://www.jamovi.org.

[57] R Core Team (2019). *R: A Language and environment for statistical computing*. (Version 3.6) [Computer software]. Retrieved from https://cran.r-project.org/.

[58] Fox, J., & Weisberg, S. (2018). *car: Companion to Applied Regression*. [R package]. Retrieved from https://cran.r-project.org/package=car.

Appendix

Detailed List of Materials/Instruments Used in Experiments

Material / Reagent / Instrument / Software	**Company**	**Order number / Model**
Compound microscope	LEICA	LEICA DM6 B
Andor iXon Ultra EMCCD	ANDOR	253.3.5/16/14996
Andor iQ 3.6.2 Software	ANDOR	
ZEISS LSM 900 with Airyscan 2	ZEISS	
ZEISS ZEN 3.0 (blue edition)	ZEISS	
Carl Zeiss microscope	CARL ZEISS	Axio Vert.A1
Pressure Supply Port	NARISHIGE	IM-400
Oil Hydraulic Micromanipulator	NARISHIGE	MMO-4
Heater	NARISHIGE	PC-100
Pure nitrogen tank	Gazsan	GA-K2099096
Fluorescence stereo microscope	LEICA	LEICA M205 FA
Stereo microscopes	LEICA	LEICA S9I
Cooled incubator	Panasonic	MIR-554-PA
Ultra-Low Temperature (UTL) freezer	Haier	DW-86L62B
Autoclave (steam sterilizer)	Tuttnauer	3850ELC-D
	Nüve steam Art	OT 90L
Laminar flow hood	Nucleon Laboratory Instruments	Class II Biosafety cabinet
PCR thermal cyclers	Thermo Fisher Scientific	ProFlex PCR System
	Bio-Rad	C1000 Touch Thermal Cycler
Waterbath	Thermo Scientific™	Precision™GP 02
	Thermo Scientific™	Precision™ GP 10
Electrophoresis	Thermo Scientific™	Owl EasyCast™ B2
	Thermo Scientific™	Owl EasyCast™ B1

	Bio-Rad	Sub-Cell Model 96
Molecular Imager®	Bio-Rad	Gel Doc™ XR+ System
Spectrophotometer	Thermo Scientific™	NanoDrop™ 2000
Centrifuge	Thermo Scientific™	MicroCL 21R Microcentrifuge
	Thermo Scientific™	MicroCL 21 Microcentrifuge
Micro centrifuges	GYROZEN	KGZS23518120872
Electronic balance	Precisa	LS 1200C SCS
	SHIMADZU	ATX 224
Vortex mixer	Stuart Biocote	SA8
Magnetic stirrers	Heidolph	MR HEI-TEC
Microwave oven	Vestel	MD 20 MB
Ice system	Scotsman	AF 80 AS 230/50/1
Water purification system	Merck	ZRQSVP800
Agar-Agar, Kobe I	CARL ROTH	5210.2 - 1 kg
Bacto™ Peptone	BD Bioscience™	211677 - 500 gr
Sodium chloride (NaCl)	ISOLAB	969.033.1000 - 1 kg
Cholesterin	CARL ROTH	8866.1 - 100 gr
Nystatin	RPI (Research Products International)	N82020-10.0
$MgSO_4.7H_2O$	CARLO ERBA REAGENTS	10034-99-8
$CaCl_2$	CARLO ERBA REAGENTS	10043-52-4
KH_2PO_4	Merck	104873.1000 - 1 kg
K_2HPO_4	Merck	105101.1000 - 1 kg
LB Broth, Miller Formulation	VWR Life Science	J106 - 1 kg
Proteinase K	Sigma-ALDRICH	SLBQ1035V
KCl	Merck	7447-40-7
Tris base	Sigma-ALDRICH	T1503 - 1 kg
$MgCl_2$	Merck	7786-30-3
10X Easy Taq buffer	TRANSBIO	N21106
High Pure dNTPs	TRANSBIO	AD101-02
Primers	MACROGEN	
Easy Taq DNA polymerase	TRANSBIO	AP111-01
Ultra pure water	Tekkim Kimya	TK.911010.0
Agarose	Prona Agarose Biomax	D00216PR
Ethidium bromide	BioShop	ETB444.1
Tris base	Sigma-ALDRICH	T1503 - 1 kg
Glacial acetic acid	ISOLAB	64-19-7
EDTA	CARLO ERBA REAGENTS	6381-92-6

100bp Plus II DNA ladder	TRANSBIO	BM321-01
6X Loading buffer	TRANSBIO	GH101-01
Bromophenol blue	AMRESCO	115-39-9
Immersion oil	Sigma-ALDRICH	56822 - 50 mL
Sodium azide	SERVA	30175.01
Halocarbon oil	Sigma-ALDRICH	H8898 - 50 mL
HEPES	BioShop	7365-45-9
Ethanol	ALKOKİM	01012018-IR.01
Injection neddle	WPI	TW100F-4
Sterile syringe (0.5mL)	AYSET Tıbbi Ürünler	KD8354-00-10/17
Sterile syringe (10mL)	Helmed	20160802
Sterile filter unit with MF-Millipore, 0.22 µm	Millex® Syringe Filters	SLGS033SS
Microscope slide	ISOLAB	I.075.05.003
Cover glass	ISOLAB	075.00.004
Parafilm	Bemis	PM-996
Pipettes 0.2-2 µl 1-10 µl 2-20 µl 10-100 µl 20-200 µl 100-1000 µl	Thermo Scientific	 PH77343 NH30094 PH79581 JH97441 JH95162 JH95573
Pipettes 10-100 µl 100-1000 µl	SCILOGEX	 YM5D071264 YM5G082883
Pipettes 0.5-10 µl 2-20 µl 10-100 µl	NICHIRYO Nichepet EX II	 J15809081 J16317571 J16101431
Multi channel pipettes 1-10 µl 10-100 µl	Thermo Scientific	 OH22524 LJ02605
Pipette tips 10 µl 200 µl 10000 µl	ISOLAB ISOLAB Biosigma	 005.01.001 005.01.002 17A0845
S1 pipet filler	Thermo Scientific	187550
Serological pipettes 10 mL 25 mL	Biosigma Biosigma	 N403346 N403347
Individual tubes (0.2 mL)	Thermo Scientific	AB-0620
Cryogen tube (2 mL)	Biosigma	CL2ARBEPSTS

Eppendorf tubes 1.5 mL 2 mL	 LAMTEK ISOLAB	 LT1003098 MTPPN6020008
Centrifuge tubes 15 mL 50 mL	 ISOLAB ISOLAB	 CTPPA7015002 CTPPA9050002
Petri dishes 60*15 mm 90*15 mm	 FIRATMED FIRATMED	 8870000046 8870000011
Weighing boats; 30 mL 100 mL	ISOLAB	 WBPSN7030001 WBPSN7100001